GLIMPSE360 Data Description

GLIMPSE360: Completing the Spitzer Galactic Plane Survey

by Marilyn R. Meade, Barbara A. Whitney, Brian L. Babler, Robert Benjamin, Ed Churchwell, Remy Indebetouw, Tom Robitaille, Martin Cohen

Version 1.5
December 18, 2014

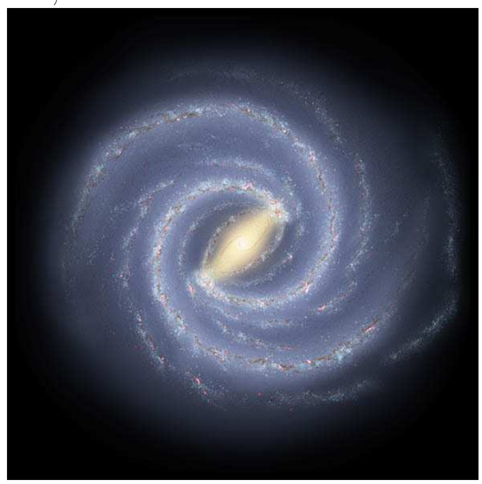

Contents

1 Quick Start

GLIMPSE360 provides mid-infrared coverage of the Outer Galaxy: longitudes l=65°-265° excluding l= 102°-109°(SMOG) and l=76°-82°(CYG-X) (see Figures 1 & 2). For those who are familiar with GLIMPSE data, GLIMPSE360 data products are very similar. There are two types of source lists: a high reliability point source Catalog and a more complete point source Archive. The other main product is the set of mosaicked images. GLIMPSE360 is a Spitzer "Warm Mission" program. After the cryogen depletion in May 2009, the observatory is operating using only IRAC's 3.6 and 4.5 μm channels.

This GLIMPSE360 data release contains images from l=64.5°-76°and 82°-102.4°. Previously l=109.0°-265.7° GLIMPSE360 images were delivered to IRSA. With this latest image delivery all of the GLIMPSE360 images have been delivered.

All of the GLIMPSE360 source lists have been delivered to IRSA. The entire GLIMPSE360 source list totals are 42,602,112 Catalog sources and 49,378,042 Archive sources. The source lists are a result of doing photometry on each IRAC frame, averaging all detections of a single band (in band-merge), then doing the merging of all wavelengths, including 2MASS J,H, and K_s, at a given position on the sky (cross-band merge). Much of the l=89.7°-102.4°data were taken during the transition period from the Cold to Warm Mission when the temperature was not stable. This resulted in calibration issues - source fluxes taken during this time are fainter than the same sources observed at a different time. The [3.6] fluxes are about 0.07 magnitudes too faint and the [4.5] fluxes about

0.03 magnitudes too faint. See Appendix A for more details.

GLIMPSE360, GLIMPSE, GLIMPSEII, GLIMPSE3D, Vela-Carina and Deep GLIMPSE data products are available at the Infrared Science Archive (IRSA)

- irsa.ipac.caltech.edu/data/SPITZER/GLIMPSE/

Two useful websites for the analysis of these data provided by the GLIMPSE team are the Web Infrared Tool Shed (WITS) and the Young Stellar Objects (YSO) Grid and Fitter

- WITS – dustem.astro.umd.edu/
- YSO Model Fitter – caravan.astro.wisc.edu/protostars/

2 GLIMPSE360 Survey and Data Products Overview

2.1 Project Overview

GLIMPSE360 is a Warm Mission Spitzer Cycle 6 Exploration Science Program (PIDs 60020, 61070, 61071, 61072, 61073, 70072) that mapped 187 degrees of longitude of the Galactic plane that have not been mapped by previous Spitzer Galactic Plane surveys (GLIMPSE, GLIMPSEII, GALCEN, GLIMPSE3D, Vela-Carina, SMOG and Cygnus-X). The specific Galactic longitudes covered by GLIMPSE360 are l=65°-76°, 82°-102°, and 109°-265°(see Figures 1 & 2). The latitude range is about 2.8°. The latitude center follows the Galactic warp (Figure 1). GLIMPSE360 completes the full circle of the Galactic plane. We refer to the previous set of Spitzer surveys as GLIMPSE and the current one as GLIMPSE360.

GLIMPSE360 uses the Spitzer Space Telescope (SST; Werner et al. 2004) Infrared Array Camera (IRAC) (Fazio et al. 2004). Warm Mission Spitzer has two IRAC bands, centered at approximately 3.6 and 4.5 μm. There are three visits on each sky position with 0.6 and 12 second frametime High Dynamic Range exposures providing a large dynamic range of sensitivity, exceeding both GLIMPSE and the Wide-field Infrared Survey Explorer (WISE; see Table 1). This differs from the previous GLIMPSE surveys which are 2-3 visit 2-sec frametime exposures, though is similar to SMOG and Cygnus-X (see Figures 1 & 2). Table 2 shows the GLIMPSE360 areas and the dates of observation for each longitude segment. All of the survey data have been taken. The GLIMPSE360 Survey produces enhanced data products in the form of a point source Catalog, a point source Archive, and mosaicked images. See Benjamin et al. (2003), Churchwell et al. (2009) and the GLIMPSE web site (www.astro.wisc.edu/glimpse/) for more description of the GLIMPSE and GLIMPSE360 projects. We are processing the SMOG and Cygnus-X data to provide consistency with our other GLIMPSE products. These teams are providing source lists as well. See the Cygnus-X website[1] for more information on their data delivery.

This document describes the data products from the GLIMPSE360 survey. The organization of this document is as follows: §2 gives an overview of the GLIMPSE360 survey, data products and complementary datasets, §3 describes the data processing; §4 discusses the quality checks and validation of the source lists; §5 provides a detailed description of the data products; and §6 describes the format. Appendix A discusses the flux calibration issues for data taken during the

[1]www.cfa.harvard.edu/cygnusX/data.html

transition from Cold to Warm operations. Appendix B gives details about the Source Quality Flag. Appendix C shows examples of artifacts remaining in our enhanced IRAC images. This document contains numerous acronyms, a glossary of which is given at the end.

Table 1. Sensitivity Limits in mJy (magnitudes in parentheses)

Project	3.6 μm Lower	3.6 μm Upper	4.5 μm Lower	4.5 μm Upper
GLIMPSE360[a]	0.021 (17.8)	1100 (6.0)	0.022 (17.3)	1100 (5.5)
WISE[b]	0.06 (16.8)	110 (8.6)	0.10 (15.6)	60 (8.6)
GLIMPSE	0.20 (15.4)	440 (7.0)	0.20 (14.9)	450 (6.5)

[a] Based on 3 visits of 0.6 & 12 second HDR frames, photometry done on individual frames

[b]WISE central wavelengths are 3.3 and 4.7 μm.

Table 2. Dates of Observations for the GLIMPSE360 Survey

longitude segment range of longitude (degrees)	dates of observation[a]
65-77	20100619-0709; 20120106-07; 20120113,14
	gaps: 20101114; 20101209-13; 20110104,05; 20111110-25
77-82.5	20100705-15; 20110707-08
82.5-90	20100708-27
	gaps: 20110723
90-102	20090903[b]-15; 20091216-17
	gaps: 20100808-27; 20100909; 20110312
109-120	20100129-0219
	gaps: 20100829-0911
120-130	20100217-0305
	gaps: 20100914,28
130-140	20100305-17
	gaps: 20101012; 20120428
140-150	20091005-16; 20100317-19
	gaps: 20101012-30; 20110413,16
150-160	20101026-1113
160-170	20100408-17; 20101107-16
	gaps: 20110413
170-180	20091027-1118; 20100426-0511; 20101113-16
	gaps: 20101114-15; 20101203-07; 20110413,14,19,24; 20111109,10,30; 20120427
180-190	20100416-0509
	gaps: 20110419,23,24
190-200	20100420-0515
	gaps: 20111130
200-210	20101203-25; 20110424-0525; 20111130
	gaps: 20120506
210-220	20110525-0607; 20120102-07; 20120506,10
220-230	20100507-30
	gaps: 20120510,18
230-240	20091203-10; 20110604-12; 20120107-10
	gaps: 20120102; 20120511,16,18; 20121230[c]
240-250	20100515-0605
	gaps: 20110524
250-255	20100605-13
255-265	20100607-17; 20110202-10
	gaps: 20120119

[a] dates in yearmoda
[b] first GLIMPSE360 observation
[c] last GLIMPSE360 observation

2.2 Data Products Overview

The GLIMPSE360 enhanced data products consist of a highly reliable Point Source Catalog (GLM360C), a more complete Point Source Archive (GLM360A), and mosaic images covering the survey area. Also provided to the astronomical community are web tools for modeling infrared data. The websites for these data products are given in §1 of this document. The enhanced data products are:

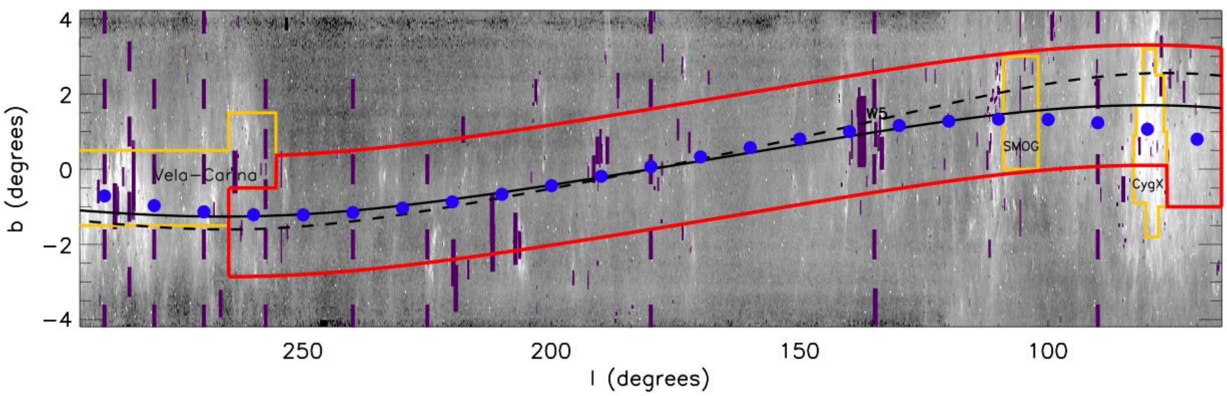

Figure 1: MSX 8 micron image of the Outer Galactic plane (Price et al. 2001). The approximate survey limits are shown with solid red lines and are based on the midplane of the CO/HI warp at a Galactocentric radius of 13 kpc (Binney & Merrifield 1998); the dashed line shows the position of the warp at 14 kpc. The filled circles show the mean latitude of red IRAS sources, binned by 10° in longitude. Rectangular boxes show regions previously observed with IRAC. In the small programs, the exact orientation of the observing strip is not shown, and is placed vertically on the figure.

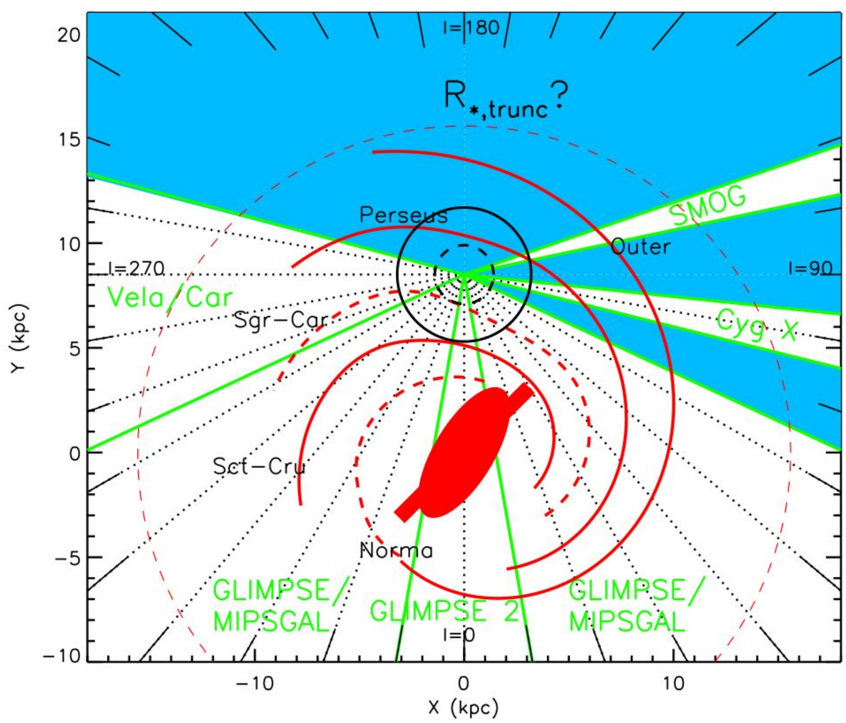

Figure 2: The Galactic Plane showing the areas covered by previous surveys in white and the GLIMPSE360 survey in blue. The approximate positions of Galactic spiral arms (Taylor & Cordes 1993) are indicated in red. The dashed spiral arms have tangency points that show no excess star counts (Benjamin 2007) and may not be "density wave" arms. The central oval and bar represent the approximate extent of the central triaxial bulge/bar (Gerhard 2002; Cole & Weinberg 2002) and the "Long" bar (Hammersley et al. 2001; Benjamin et al. 2005). The radius marking the expected truncation or break in the exponential Galactic stellar disk is also shown with a dashed line.

1. The GLIMPSE360 Catalog (GLM360C, or the "Catalog") consists of the highest reliability point sources. See §3.4 for a discussion of the Catalog criteria. Figure 3 shows the number of GLIMPSE360 Catalog sources as a function of magnitude for the two IRAC bands. For each IRAC band the Catalog provides fluxes (with uncertainties), positions (with uncertainties), the areal density of local point sources, the local sky brightness, and a flag that provides information on source quality and known anomalies present in the data. Sources were band-merged with the Two Micron All Sky Survey Point Source Catalog (2MASS; Skrutskie et al. 2006). 2MASS provides images at similar resolution to IRAC, in the J (1.25 μm), H (1.65 μm), and K_s (2.17 μm) bands. For each source with a 2MASS counterpart, the GLM360C also includes the 2MASS designation, counter (a unique identification number), fluxes, signal-to-noise, and a modified source quality flag. For some applications, users will want to refer back to the 2MASS Point Source Catalog for a more complete listing of source information. The GLIMPSE360 Catalog format is ASCII, using the IPAC Tables convention (irsa.ipac.caltech.edu/applications/DDGEN/Doc/ipac_tbl.html).

2. The GLIMPSE360 Archive (GLM360A or the "Archive") consists of point sources with less stringent selection critera than the Catalog (§3.4). The information provided is in the same format as the Catalog. The number of Archive sources as a function of magnitude for each IRAC band is shown in Figure 3. The Catalog is a subset of the Archive, but the entries for a particular source might not be the same due to additional nulling of magnitudes in the Catalog because of the more stringent requirements (§3.4).

3. The GLIMPSE360 Image Atlas comprises mosaicked images for each band, each covering e.g. $3.1^\circ \times 3.6^\circ$with $1.2''$ pixels. These are 32-bit IEEE floating point single extension FITS formatted images covering the survey area. These images are in units of surface brightness MJy/sr. Mosaics of each band are also made for smaller e.g. $1.1^\circ \times 1.1^\circ$ areas, with a pixel size of $0.6''$. The $1.2''$ pixel mosaics are provided with and without background matching and gradient correction. The background matching and gradient correction process (§3.1) may be removing real sky variations so we provide these images *in addition* to the images that do not have the background matching. Also included are quicklook 3-color jpeg images (IRAC [3.6], IRAC [4.5] and WISE [12]) of the same size as the FITS images.

4. The Web Infrared Tool Shed (WITS) is a web interface to a collection of models of IR spectra of dusty envelopes and photodissociation regions (PDRs), updated for IRAC and MIPS band passes. WITS is described in detail in §5.3.

5. The YSO Model Grid and Fitter is a web-based home of a large grid of 200730 YSO model spectral energy distributions (SEDs). The 2-D YSO radiation transfer models of YSOs producing SEDs span a large range of evolutionary stages and stellar masses. The model grid browser allows users to examine SED variations as a function of a range of physical parameters. An online fitting tool fits input data using the grid of model SEDs. The Grid and Fitter are described in §5.4.

2.3 Complementary Datasets

Numerous complementary datasets will increase the scientific impact of the Spitzer Galactic Plane Surveys. We list several of these surveys here along with links to their websites.

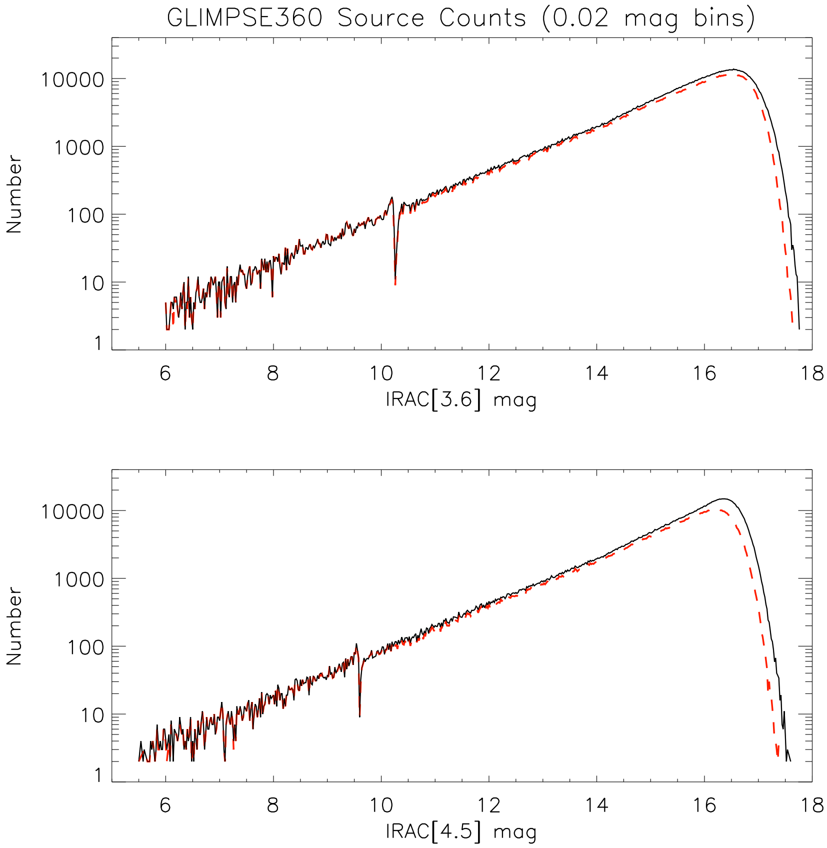

Figure 3: GLIMPSE360 Catalog and Archive source counts versus magnitude for IRAC [3.6] & [4.5]. The dashed red lines are the Catalog; the black solid lines are the Archive. Included are all the GLIMPSE360 data. The glitch in the [3.6] plot at 10.25 and the [4.5] plot at 9.6 are at the boundary where either the 0.6 sec FT data or the 12 sec FT data are used for photometry (see §3.3).

1. 2MASS (Skrutskie et al. 2006; irsa.ipac.caltech.edu/Missions/2mass.html) provides imaging at similar resolution to IRAC, in the J (1.25 μm), H (1.65 μm), and K_s (2.17 μm) bands for the entire sky.

2. The Midcourse Space Experiment (MSX) (Price et al. 2001; irsa.ipac.caltech.edu/Missions/msx.html) observed the Galactic plane in several mid-IR wavebands (from 4.2 to 26 μm) with 18″ resolution at 8 μm.

3. Herschel Infrared Galactic Plane Survey (HI-GAL and HI-GAL360) (Molinari et al 2010) (herschel.esac.esa.int/ and http://www.ipac.caltech.edu/project/41) cover the same areas as the Spitzer Galactic plane surveys (GLIMPSE et al.), with wavelength coverage from 70 - 500 μm.

4. Wide-field Infrared Survey Explorer (WISE) is an all-sky survey from 3.4 to 22 μm (wise.ssl.berkeley.edu/; Wright et al 2010).

5. AKARI infrared survey (Ishihara et al 2010; irsa.ipac.caltech.edu/Missions/akari.html) is an all-sky infrared survey from 1.8 to 180 μm.

6. UKIDSS-GPS (UKIRT Infrared Deep Sky Survey Galactic Plane Survey) is a near-IR Galactic plane survey (Lucas et al 2008) (www.ukidss.org/) in J, H & K_s.

7. VVV (Vista Variables in the Via Lactea) Minniti et al 2010 (http://mwm.astro.puc.cl/mw/) is an ESO near infrared variability survey of the Milky Way bulge and an adjacent section of the mid-plane in bands Z, Y, H, J and K_s).

8. UWISH2 (UKIRT Widefield Infrared Survey for H2, Froebrich et al 2010) (astro.kent.ac.uk/uwish2/) is imaging about 150 square degrees along the Galactic plane ($10° < l < 65°$; $-1° < b < +1°$) with WFCAM at UKIRT. The observations are taken with the narrow band filter centered on the molecular hydrogen 1-0 S(1) emission line at 2.122 μm.

9. Submillimetre Common-User Bolometer Array 2 (SCUBA-2) is an all-sky survey in the sub-millimeter (200 μm to 1 mm)(http://www.jach.hawaii.edu/JCMT/continuum/) (MacKenzie et al 2011; Holland et al 2006).

10. Galactic Australian SKA Pathfinder Survey (GASKAP) (www.atnf.csiro.au/research/GASKAP/) (Dickey et al. 2010) is a high spectral resolution ($20''$) study of the HI and OH lines in the Milky Way and Magellanic Systems. It will achieve about an order of magnitude improvement in both brightness sensitivity and in angular resolution.

11. Five-College Radio Astronomy Observatory (FCRAO) CO surveys of the Outer Galaxy (l=102°-141°, Heyer et al 1998; l=55°-102°, Mottram & Brunt 2010. www.astro.umass.edu/∼fcrao/) have a spatial resolution of $45''$ and a spectral resolution of about 0.15 km/s.

12. Milky Way Galactic Ring Survey (GRS) (www.bu.edu/galacticring), a Boston University and Five College Radio Astronomy Observatory collaboration, is a large-scale ^{13}CO line survey of the inner Galaxy between longitudes 18° and 52° (Jackson et al 2006). Compared with previous molecular line surveys of the inner Galaxy, the GRS offers excellent sensitivity (<0.4 K), higher spectral resolution (0.2 $\mathrm{km\,s^{-1}}$), comparable or better angular resolution ($46''$) and sampling ($22''$), and the use of ^{13}CO (1-0), a better column density tracer than the commonly observed ^{12}CO (1-0) line.

13. Arecibo and Green Bank Telescope (GBT) surveys of IR-color selected H II Regions in the GLIMPSE survey region: a dataset that resolves distance ambiguities to massive star formation regions. More than 100 IR-color selected H II regions have been observed with the Arecibo 300m and NRAO Green Bank Telescope in the H110α and H_2CO ($1_{10} - 1_{11}$) lines to resolve distance ambiguities. The H110α line determines the kinematic distance and the H_2CO ($1_{10} - 1_{11}$) absorption line resolves the near-far distance ambiguity. In 2001 this technique was applied as a pilot project at Arecibo to 20 Ultra-Compact (UC) H II regions. Distances were successfully determined for 19 sources (Araya et al. 2002). In 2002 H110α was detected toward 45 UC H II regions and the near-far distance ambiguity resolved for 35 objects; ten were found to lie near the tangent point (Watson et al. 2003). H110α and H_2CO ($1_{10} - 1_{11}$) data have been obtained for an additional 72 compact HII regions using the NRAO GBT telescope.

14. The International Galactic Plane Survey (www.ras.ucalgary.ca/IGPS) is an H I 21-cm survey of the disk of the Milky Way. This survey provides data cubes of the H I spectral line

emission with resolution of $1'$ and one km/s over the entire area of the GLIMPSE survey. It also provides continuum maps of the Stokes *I, Q, U*, and *V* emission.

15. The Coordinated Radio and Infrared Survey for High-Mass Star Formation (CORNISH) (Hoare et al. 2012) (www.ast.leeds.ac.uk/Cornish/index.html) Very Large Array (VLA) 6 cm continuum survey of much of the Galactic plane. CORNISH has a spatial resolution of $\sim 1''$ and a sensitivity of $\sim$1 mJy, very similar to that of IRAC. This survey will cover the longitude range l= -20° to 66°, b < |1|°. It is imaging SNRs, HIIs, PNs and galaxies.

16. The Galaxy ALFA Low Latitude HI Survey (GALFA) (http://www.naic.edu/alfa/galfa/; Stanimirovic et al 2006) is mapping H I in the Milky Way Galaxy with the Arecibo 305-meter telescope.

17. The Bolocam Galactic Plane Survey (BGPS) (http://milkyway.colorado.edu/bgps/; Aguirre et al 2011) is a 1.1 mm continuum survey of 170 square degrees of the Galactic plane visible from the northern hemisphere. The survey is contiguous over the range -10.5°< l < 90.5°, $|b| < 0.5°$. Towards the Cygnus X region, the coverage was flared to $|b| < 1.5°$over the range 75.5°< l < 87.5°. In addition, cross-cuts to $|b| < 1.5°$were made at l=3°,15°,30°, and 31°. Four targeted regions in the outer Galaxy were also observed, covering l=111°near NGC 7538, the W3/4/5 complex, IC1396, and the Gem OB1 complex.

18. The APEX Telescope Large Area Survey of the Galaxy (ATLASGAL) http://www3.mpifr-bonn.mpg.de/div/atlasgal/), is an observing program with the LABOCA bolometer array at APEX, located in Chile. It mapped over 400 square degrees at 870 microns in the inner Galaxy.

3 Pipeline Processing

3.1 Image Processing

Image processing steps for photometry include masking hot, dead, and missing data pixels (using SSC supplied flags). Pixels associated with saturated stars are masked using an algorithm generated by GLIMPSE; this algorithm finds most of the saturated stars. Pixels within a PSF-shaped region (with a 24-pixel radius) of a saturated source are flagged. Several image artifacts (described in Hora et al (2004) and the IRAC Data Handbook[2]) are corrected for in the GLIMPSE pipeline. A description of the Spitzer Warm Mission IRAC image features is found at irsa.ipac.caltech.edu/data/SPITZER/docs/irac/warmfeatures/. We correct for column pulldown[3] in bands [3.6] & [4.5], using an algorithm written by Matt Ashby and Joe Hora of the IRAC instrument team [4] and modified by GLIMPSE to handle variable backgrounds. There is no muxbleed effect in the Warm Mission IRAC frames.

Image processing for the mosaic image products include the column pulldown correction mentioned above. Hot, dead, and missing pixels are masked. Outlier masking (e.g. cosmic rays, stray light from bright sources outside the field of view;rmask) was done using IRACproc (Schuster et al 2006). The instrument artifacts found by visual inspection of the higher resolution $0.6''$ mosaics

[2]irsa.ipac.caltech.edu/data/SPITZER/docs/irac/iracinstrumenthandbook

[3]Column pulldown is a reduction in intensity of the columns in which bright sources are found in bands [3.6] and [4.5]. See Warm *Spitzer* Observers Manual (Warm SOM) at ssc.spitzer.caltech.edu/warmmission/propkit/som/.

[4]irsa.ipac.caltech.edu/data/SPITZER/docs/dataanalysistools/tools/contributed/irac/fixpulldown/

were removed. Latent images from bright sources are removed when possible. If there are areas of overlapping image artifacts that cause a gap in coverage, we do not mask that area. Latent images can repeat (particularly along rows and columns) and remain in the images because masking them would cause gaps in coverage. See Appendix C for examples of instrument artifacts that can still be found in the images after the outlier masking and visual inspection stray light removal was done. See SSC's IRAC image features web sites[5], [6] and the IRAC Data Handbook for more information about the detector artifacts. We use the Montage[7] package v3.0 to mosaic and project to Galactic coordinates.

We match instrumental background variations between the IRAC frames using Montage's level background correction algorithm[8]. Instrument artifacts such as full array pull-up, frame pull-down and offsets between AORs are mostly removed from the images. See Appendix C for an example of a [3.6] image that was not background matched (Figure 13) and that same image, Figure 14, that was background matched and gradient corrected. Offsets between AORs and full array pull-ups have been mitigated. In the background matching process, Montage introduces unwanted large-scale gradients. Our gradient correction algorithm finds the large-scale gradients by taking the corrections table produced by Montage and creating a smoothed version to eliminate small-scale corrections. This is done by using a Radial Basis Function interpolation with a smoothing factor of 1000. We then find the difference between the corrections and the smoothed corrections, find the standard deviation of this difference, then reject all points which deviate by more than 5 sigma. A new smoothed correction map is computed and the process is repeated until no points are rejected (typically 10 iterations). Once this is complete, a final correction map is computed and removed from the image, thus undoing the large-scale gradients introduced by Montage. The background matching and gradient correction may be removing real sky variations so we provide these images *in addition* to the images that do not have the background matching.

3.2 Photometry

We use a modified version of DAOPHOT (Stetson 1987) as our point source extractor, performing Point Spread Function (PSF) fitting on individual IRAC frames. We repeat the photometry calculations on the residual (point-source removed) images (referred to as "tweaking" in Table 5), which has been shown to substantially improve the flux estimates in complex background regions. More details about the photometry steps can be found at www.astro.wisc.edu/glimpse/glimpse_photometry_v1.0.pdf. The warm mission array-location-dependent photometric corrections[9] were applied to the source lists.

[5] irsa.ipac.caltech.edu/data/SPITZER/docs/irac/features/

[6] irsa.ipac.caltech.edu/data/SPITZER/docs/irac/warmfeatures/

[7] montage.ipac.caltech.edu/;Montage is funded by the National Aeronautics and Space Administration's Earth Science Technology Office, Computation Technologies Project, under Cooperative Agreement Number NCC5-626 between NASA and the California Institute of Technology. Montage is maintained by the NASA/IPAC Infrared Science Archive.

[8] montage.ipac.caltech.edu/docs/algorithms.html#background

[9] section 3.5 of http://irsa.ipac.caltech.edu/data/SPITZER/docs/irac/warmfeatures/

3.3 Bandmerging to Produce Source Lists

The point source lists are merged at two stages using a modified version of the SSC bandmerger[10]. Before the first stage, source detections with signal-to-noise (S/N) less than 3 are culled. During the first stage, or in-band merge, all detections at a single wavelength are combined using position, S/N and flux to match the sources. The 0.6 second flux is included if the signal-to-noise is greater than (5,5) and the magnitudes are brighter than (10.25, 9.6) for the two IRAC bands [3.6] and [4.5], respectively. This prevents Malmquist bias for the 0.6 second data from affecting the results. The 12 second flux is included if the magnitude is fainter than (10.25, 9.6) for the IRAC bands [3.6] and [4.5], respectively. Fluxes of sources within $1\overset{''}{.}6$ in the IRAC frame are combined together or "lumped" into one flux.

The second stage, or cross-band merge, combines all wavelengths for a given source position using only position as a criterion in order to avoid source color effects. Cross-band lumping is done with a $1\overset{''}{.}6$ radius. Position migration can still occur in the bandmerging process which results in a small number of sources that are within $1\overset{''}{.}6$ of another source. In the cross-band merge stage we also merge with the All-Sky 2MASS (Skrutskie et al 2006) point source list. Note that we only propagate a subset of the 2MASS quality flags and information, and users should refer to the original 2MASS catalog available through IRSA for full information. We include the unique numeric identifier assigned by the 2MASS project "cntr" (tmasscntr in the GLIMPSE360 source lists) to allow this cross-referencing.

3.4 Source Selection for Catalog and Archive

Now we describe the selection criteria for the Catalog and Archive once photometry and bandmerging have been completed. These criteria were established to produce high reliability single frame photometry where the abundance of cosmic rays can contribute to false sources.

The Catalog is a more reliable list of sources, and the Archive is a more complete list both in number of sources and flux measurements at each wavelength (less nulling of fluxes). The main differences between the Catalog and Archive are 1) fluxes brighter than a threshold that marks a nonlinear regime are nulled (removed) in the Catalog; 2) sources within 2.0″ of another are culled (removed) from the Catalog, whereas the Archive allows sources as close as $0\overset{''}{.}5$ from another; 3) sources within the PSF profile of a saturated source are culled from the Catalog but not the Archive; and 4) the Catalog has higher signal-to-noise thresholds and slightly more stringent acceptance criteria (e.g., number of detections in various bands) . Users who want a more "bullet-proof" list and don't want to have to get as familiar with the source quality flags, or who will be doing the kind of analysis that does not allow for manual inspection of very many source Spectral Energy Distributions (SEDs), should use the Catalog. Users who want more complete SEDs and source lists, and are willing to invest time to understand the source quality flags, can make use of the Archive. This allows the use of lower limits for fluxes that are nearly saturated, more data points at lower signal-to-noise, more sources in crowded regions, and more sources in the wings of saturated sources. Using the source quality flag, these sources can be identified and should be more carefully inspected to verify their quality. Both Archive and Catalog users can improve the quality of their data by paying attention to the source quality flag (§5.1.6 and Appendix B), as well as other diagnostic information such as the close source flag (see §5.1.6).

[10]ssc.spitzer.caltech.edu/dataanalysistools/tools/bandmerge/

Our source list criteria have been developed to ensure that each source is a legitimate astronomical source (*culling* criteria) and that the fluxes reported for the IRAC bands are of high quality (*nulling* fluxes if they do not meet quality standards).

3.4.1 Culling Criteria - is it a real source?

The IRAC source lists were produced from photometry on individual BCD frames. The 12 second exposures suffer from cosmic rays. For this reason, stringent selection criteria were developed to limit false sources. To ensure high reliability of the final point-source Catalog (GLM360C) by minimizing the number of false sources, we adopt the following selection criteria: Given M detections out of N possible observations (see §5.1.5), we require that $M/N \geq 0.6$ in one band (the selection band), and $M/N \geq 0.32$ in an adjacent band (the confirming band), with a $S/N > 5$ for IRAC bands [3.6] and [4.5]. The 2MASS K_s band is counted as a detection. As an example, a source is typically observed three times at 0.6 second frametime and three times at 12 second frametime for a total of six possible observations in each band. Such a source detected four times in band [3.6] with $S/N > 5$, and twice in band [4.5] with $S/N > 5$ would be included in both the Catalog and Archive. For a typical source, extracted from 3×12 sec frametime images, the minimum detection criterion ($M/N \geq 0.32$) amounts to being detected twice in one band and once in an adjacent band. Thus, we sometimes refer to this as the 2+1 criterion. In our source selection process, we don't allow fluxes in bands with hot or dead pixels within 3 pixels of source center, those in wings of saturated stars, and/or those within 3 pixels of the frame edge. Sources are also culled when they are too close to another source because this neighboring source could influence the flux for the source: We use the Archive list to search for near neighbors, and cull from the Catalog sources within $2''$.

For the Archive (GLM360A), the culling criteria are less stringent. The M/N and S/N criteria are the same as for the Catalog to limit false sources caused by cosmic rays. The close source criteria is relaxed: Sources are removed from the Archive if there are neighboring Archive sources within $0.''5$ of the source.

3.4.2 Nulling Criteria - ensuring high quality fluxes

To ensure high quality fluxes for each source, a flux/magnitude entry for a band in the *Catalog* will be nulled, i.e. removed, for any of the four following reasons: 1) the source is brighter than the 0.6 sec. saturation magnitude limits, 6.0 and 5.5 for IRAC bands [3.6] and [4.5], respectively; 2) the source location is flagged as coincident with a bad pixel; 3) the S/N is less than 6 for IRAC bands [3.6] and [4.5] in order to mitigate Malmquist bias; 4) for 12-second only data, if $M < 2$ or M/N is less than 0.6 in order to mitigate faint cosmic ray detections. If all fluxes for a source are nulled, the source is removed from the Catalog.

For the *Archive*, the nulling criteria are less stringent. The magnitude is nulled if the S/N is less than 5 in that band. For photometry with 12 second only data, if $M/N < 0.3$ the magnitude is nulled.

The actual null values for the fields in the entry for a source are given in Table 8.

Since the selection (or culling) criteria are fairly similar between the Catalog and Archive, the total number of sources is not that different. However, the Catalog sources have more fluxes nulled.

4 Quality Checks and Source List Validation

We summarize here analysis used to validate the Catalog and Archive point source lists. Additional information can be found in documents at www.astro.wisc.edu/glimpse/docs.html. A study of completeness in all the GLIMPSEs point source lists can be found in Kobulnicky et al. 2013.

4.1 Astrometric Accuracy

Sources bright enough to have 2MASS associations are typically within 0.3″ of the corresponding 2MASS position, as discussed in §5.1.3. Figure 4 shows a comparison of GLIMPSE360 source positions to the 2MASS PSC positions, in 0.02″ bins, for an eight degree longitude, three degree wide latitude area in the GLIMPSE360 survey. The peak of the plot is at 0.1″ and the majority of the sources have positional differences less than 0.3″ , similar to previous GLIMPSE source lists. Fainter GLIMPSE360 sources are likely to have larger errors due to poorer centroiding.

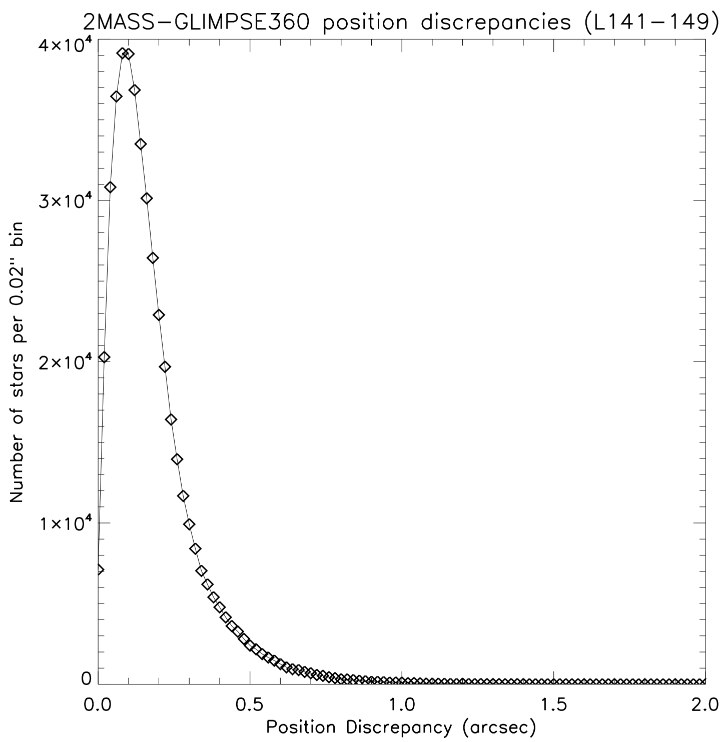

Figure 4: Comparison of GLIMPSE360 source positions to their corresponding 2MASS PSC positions from sources from longitudes between 141°and 149° and latitudes from about -1.15°to +2.65°. The astrometric discrepancy plotted is the angular separation in arcseconds between the GLIMPSE360 position and the 2MASS position. Note that sources with 2MASS associates have GLIMPSE360 positions that are in part derived from the 2MASS position. Thus this is not a comparison of a pure IRAC-only position with the 2MASS position.

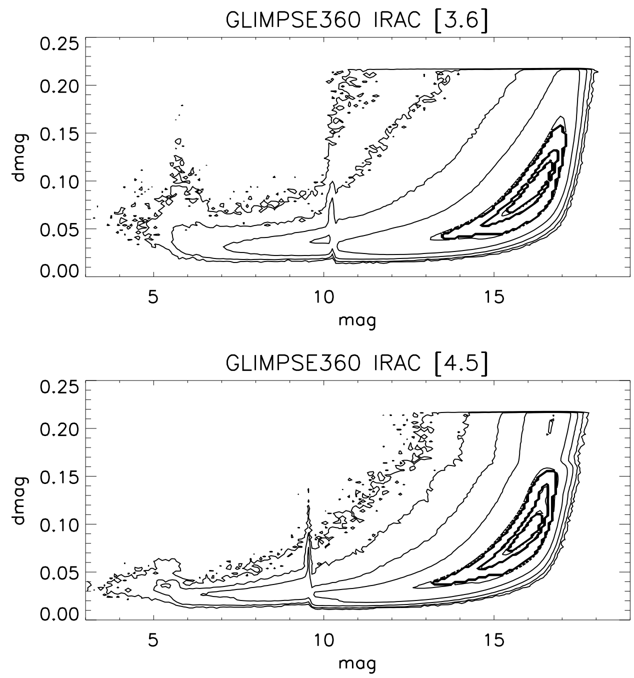

Figure 5: Magnitude uncertainty vs. magnitude for each IRAC band included in the GLIMPSE360 Archive for the entire survey area. Contours show the density of sources. The lack of data above dmag of 0.22 is caused by the criterion that Archive data have signal to noise ratios of 5 or better. The "bump" at [3.6]=10.25 and [4.5]=9.6 is the boundary where the 0.6 sec frametime data are used for brighter sources and the 12 sec frametime data are used for fainter sources.

4.2 Precision and Accuracy of the Photometry

Figure 5 shows the photometric uncertainty for the entire GLIMPSE360 survey region. There is a jump in uncertainties at the brighter magnitudes which shows the boundary between the 0.6 and 12 sec frametime photometry (with shorter exposures having larger errors).

The reliability of the flux uncertainities was studied by comparing the quoted error (dFi) with the root mean square (RMS) of the measurements (Fi_rms) for thousands of sources in a given flux range; if a large fraction of the sources have intrinsic variability, this method will produce an upper limit to the uncertainties. The DAOPHOT output uncertainties include a PSF fitting component, photon noise, read noise, and goodness of flat fielding; the strength of each component is not perfectly determined. Based on our comparison to the RMS of the measurements, we have decreased our photometry uncertainties produced by DAOPHOT by 5% in the [3.6] band and 35% in the [4.5] band.

Photometric accuracy was further verified by comparison with about 14 flux calibrators distributed in the GLIMPSE360 survey region. The flux predictions were supplied by Martin Cohen. These calibrators span a range of fluxes in each IRAC band. The techniques used to produce the flux predictions are described in Cohen et al. (2003). Our analysis is applied on the calibrators fainter than the saturation limit that are extracted without confusion. Figure 6 shows the agreement between the GLIMPSE360 magnitudes and the predicted magnitudes. Uncertainties in both the extracted and predicted magnitudes were added in quadrature to produce the plotted error bars.

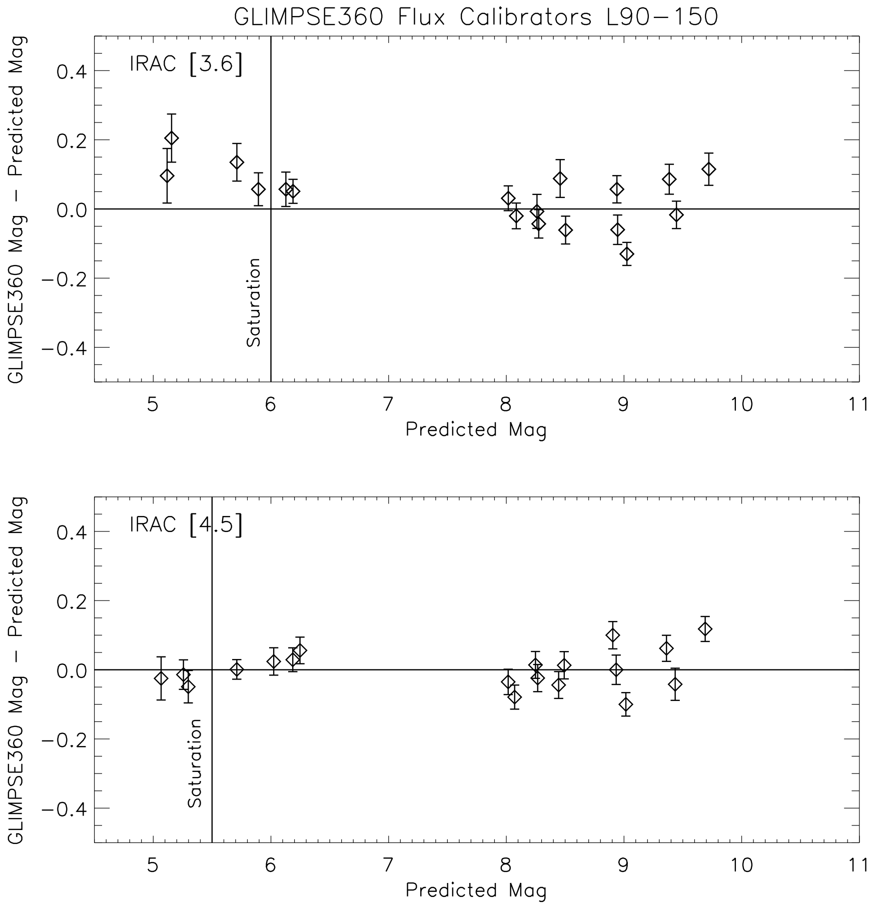

Figure 6: Comparison of GLIMPSE360 flux calibrators to predictions provided by Martin Cohen for each IRAC band. Error bars are the root-sum-of-squares of the errors of both the extracted and predicted magnitudes for each source. The vertical lines are the best estimates of the saturation limits.

Table 3 gives details about the number of flux calibrators used for each band (which varies due to saturation and partial coverage on the survey boundaries), average differences (GLIMPSE360 magnitude minus the predicted magnitude), and RMS errors.

Table 3. Comparison of Flux Calibrators to Predicted Magnitudes

Band (μm)	[3.6]	[4.5]
No. Flux calibrators	14	16
Ave. [Observed-Predicted] mag	0.010500	0.005813
RMS error	0.067448	0.058035

4.3 Color-Color and Color-Magnitude Plots

Color-color and color-magnitude plots were made of the Catalog and Archive files (in approximately $4^{\circ}\times$ 3° regions). An example set of color-color and color-magnitude plots is shown in Figures 7

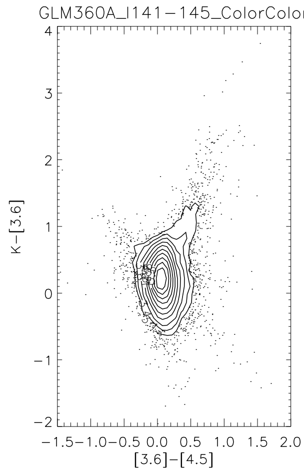

Figure 7: Color-color plot of the region $l = 141° - 145°$ and $b = -1.15°\ to + 2.65°$ for sources in the Archive. 10 contours are evenly spaced between log(# sources/mag^2)=2.0 and the log of maximum number of sources per square magnitude. The contours are labeled with the log of the number of sources per square magnitude. Outside of the lowest contour, the positions of individual sources are plotted.

& 8, respectively. The color-color plots generally show a peak near 0 color due to main sequence and giant stars. The outliers in Figure 7 (the points) comprise 0.4% of the sources. Sources with these unusual colors usually either have intrinsic color variations due to e.g., dust scattering or emission; or have poor flux extractions. The color-magnitude plots can be used to show the limiting magnitudes where the flux uncertainties become large and the colors begin to show large deviations. This is not significant in Figure 8 which demonstrates that our fluxes are accurate at the faint end. Postscript files of the color-color and color-magnitude plots for source lists for each set of 4 degrees of longitude in the entire GLIMPSE360 survey are available from the GLIMPSE360 web site (www.astro.wisc.edu/glimpse/glimpse360/ColorColor/ and www.astro.wisc.edu/glimpse/glimpse360/ColorMag/).

4.4 Other checks

Spot checks include inspection of residual images to verify proper point source extraction; overplotting the positions of the sources in the Catalogs and Archives on mosaic images; and plotting Spectral Energy Distributions (SEDs) of several sources. In addition to these and other tests described in previous documents, our source lists have been extensively tested by users analyzing the data on evolved stars, YSOs, and other sources throughout the Galaxy and the Magellanic Clouds (GLIMPSE, SAGE-LMC, SAGE-SMC).

5 Data Products Description

5.1 Catalog and Archive Fields and Flags

Each entry in the GLIMPSE360 Catalog and Archive has the following information:

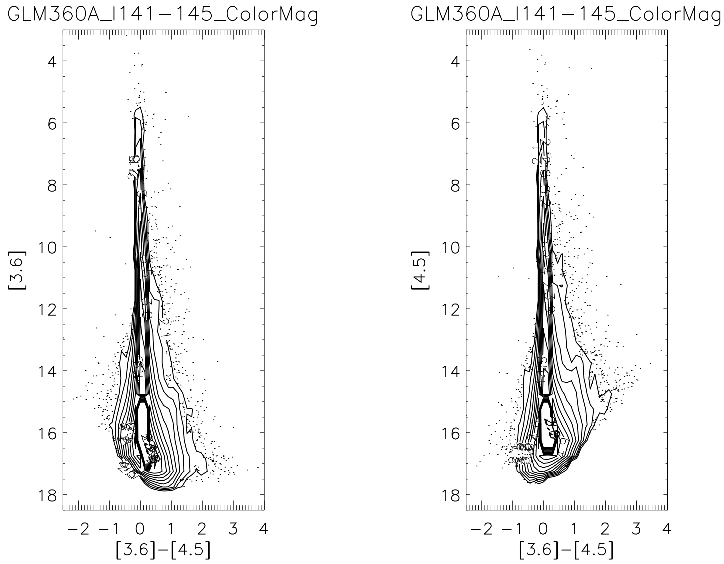

Figure 8: Same as Figure 7 except that these are Color-magnitude plots.

designation	SSTGLMC GLLL.llll±BB.bbbb, SSTGLMA GLLL.llll±BB.bbbb
2MASS PSC names	2MASS designation, 2MASS counter
position	l, b, dl, db, ra, dec, dra, ddec
flux	mag_i, dmag_i, F_i, dF_i, F_i_rms (IRAC)
	mag_t, dmag_t, F_t, dF_t (2MASS)
diagnostic	sky_i, SN_i, $\mathrm{srcdens}_i$, # detections M_i out of N_i possible (IRAC)
	SN_t (2MASS)
flags	Close Source Flag, Source Quality Flag (SQF_i), Flux Method Flag (MF_i) (IRAC)
	Source Quality Flag (SQF_t) (2MASS)

where i is the IRAC wavelength number (IRAC bands 3.6, 4.5, 5.8 and 8.0 μm) and t is the 2MASS wavelength band (J, H, K_s). For the GLIMPSE360 Warm Mission data, bands [5.8] and [8.0] fields are always nulled since no data were taken at those wavelengths. We keep the same format as the previous GLIMPSE source lists.

Details of the fields are as follows:

5.1.1 Designation

This is the object designation or "name" as specified by the IAU recommendations on source nomenclature. It is derived from the coordinates of the source, where G denotes Galactic coordinates, LLL.llll is the Galactic longitude in degrees, and ±BB.bbbb is the Galactic latitude in degrees. The coordinates are preceded by the acronym SSTGLMC (GLIMPSE Catalog) or SSTGLMA (GLIMPSE Archive).

5.1.2 2MASS PSC information

The 2MASS designation is the source designation for objects in the 2MASS All-Sky Release Point Source Catalog. It is a sexagesimal, equatorial position-based source name of the form hhmmssss±ddmmsss, where hhmmssss is the right ascension (J2000) coordinate of the source in hours, minutes and seconds, and ±ddmmsss is the declination (degrees, minutes, seconds). The 2MASS counter is a unique identification number for the 2MASS PSC source. See www.ipac.caltech.edu/2mass/releases/allsky/doc/sec2_2a.html for more information about these fields.

5.1.3 Position

The position is given in both Galactic (l, b) and equatorial (α, δ) J2000 coordinates, along with estimated uncertainties. The pointing accuracy is $1''$ (Werner et al. 2004). The SSC pipeline does pointing refinement[11] of the images based on comparison with the 2MASS Point Source Catalog, whose absolute accuracy is typically $< 0.2''$ (Cutri et al. 2005). After applying the SSC geometric distortion corrections and updating to the 2MASS positions, the GLIMPSE point source accuracy is typically $\sim 0.3''$ absolute accuracy, limited by undersampling of the point-spread function. The position uncertainties are calculated by the bandmerger based on the uncertainties of individual detections, propagated through the calculation of the weighted mean position. Sources with 2MASS associates have positions in part derived from the 2MASS position.

5.1.4 Flux

For each IRAC band i = 3.6 and 4.5 μm and, when available 2MASS band t = J, H, and K_s, the fluxes are expressed in magnitudes (mag_i, mag_t) and in mJy (F_i, F_t). Each IRAC flux is the error-weighted average of all independent detections of a source. The 2MASS magnitudes and uncertainties are from the 2MASS All-Sky Release Point Source Catalog. They are the j_m, j_msigcom, h_m, h_msigcom, and k_m, k_msigcom columns from the 2MASS PSC. The zeropoints for converting from flux to magnitude are from Reach et al (2005) for the IRAC bands and Cohen et al. 2003 for 2MASS and given in Table 4.

Table 4. Zeropoints for Flux to Magnitude Conversion

Band	J	H	K_s	[3.6]	[4.5]	[5.8]	[8.0]
Zeropoints (Jy)	1594	1024	666.7	280.9	179.7	115.0	64.13

The IRAC flux/magnitude uncertainties (dF_i; $dmag_i$) are computed during the photometry stage and take into account photon noise, readnoise, goodness of flat fielding, and PSF fitting (Stetson 1987).

The rms deviation (F_i_rms) of the individual detections from the final flux of each source is provided. The F_rms is calculated as follows: F_rms=$\sqrt{\sum (F_j - < F >)^2/M}$ where j is an individual IRAC frame, $< F >$ is the average Flux, and M is the number of detections.

5.1.5 Diagnostics

The associated flux diagnostics are a local background level (sky_i) (i = 3.6 and 4.5 μm) in MJy/sr, a Signal/Noise (SN_i), a local source density ($srcdens_i$) (number of sources per square arcmin), and number of times (M_i) a source was detected out of a calculated possible number (N_i). The

[11] irsa.ipac.caltech.edu/data/SPITZER/docs/irac/iracinstrumenthandbook/50/#_Toc296497447

Signal/Noise is the flux (F_i) divided by the flux uncertainty (dF_i). The Signal/Noise for the 2MASS fluxes (SN_t) have been taken from the 2MASS PSC (the j_snr, h_snr and k_snr columns). The local source density is measured as follows: The individual IRAC frame is divided into a 3×3 grid, each of the nine cells being $1.71'$ x $1.71'$. A source density is calculated for each cell (number of sources per arcmin^2), and is assigned to each source in that cell. The local source density can be used to assess the confusion in a given region, along with the internal reliability. M_i and N_i can be used to estimate reliability. N_i is calculated based on the areal coverage of each observed frame; due to overlaps some areas are observed more often per band.

Detections (M) can be thrown out by exposure time (when combining 0.6 and 12 second frametime data, for example), or because they have bad SQF flags. Detections are also thrown out at the beginning of bandmerging for sensitivity or saturation reasons. If *any* detections without bad flags went into the final flux, then only those good detections are counted. If all detections had bad flags, then all are counted, and the final source will have some bad quality flags also. Bad in this context is 8=hot/dead pixel and 30=edge (see §5.1.6 and Appendix B for SQF details). N is all frames containing the position of the combined source in this band (*not* including the edge of the frame, within 3 pixels) for which the exposure time was used in the final flux. As for M, if *any* good detections are used, we only count the good detections, but if they're all bad we count all of them and set flags in the final source. For sources not detected in a band, the position of the final cross-band merged source is used for calculating N.

5.1.6 Flags

There are three types of flags: the Close Source Flag, the Source Quality Flag and the Flux Calculation Method Flag. The Close Source Flag is set if there are Archive sources that are within $3''$ of the source. The Source Quality Flag provides a measure of the quality of the point source extraction and bandmerging. The Flux Calculation Method Flag describes how the final Catalog/Archive flux was determined.

• The Close Source Flag is set when a source in the Archive is within $3.0''$ of the source. It was found that the magnitudes of a source with nearby sources closer than about $2''$ are not reliably extracted and bandmerged. A source that has Archive sources within $2.0''$ of the source are *culled* from the Catalog. A source that has Archive sources within $0.5''$ of the source are *culled* from the Archive. The flag is defined as follows:

0=no Archive source within $3.0''$ of source
1=Archive sources between $2.5''$ and $3.0''$ of source
2=Archive sources between $2.0''$ and $2.5''$ of source
3=Archive sources between $1.5''$ and $2.0''$ of source
4=Archive sources between $1.0''$ and $1.5''$ of source
5=Archive sources between $0.5''$ and $1.0''$ of source
6=Archive sources within $0.5''$ of source

• The Source Quality Flag (SQF) is generated from SSC-provided masks and the GLIMPSE pipeline, during point source extraction on individual IRAC frames and bandmerging. Each source quality flag is a binary number allowing combinations of flags (bits) in the same number. Flags are set if an artifact (e.g., a hot or dead pixel) occurs near the core of a source - i.e. within ∼3 pixels. A non-zero SQF will in most cases decrease the reliability of the source. Some of the bits, such as the DAOPHOT tweaks, will not compromise the source's reliability, but has likely increased the uncertainty assigned to the source flux. If just one IRAC detection has the condition requiring a bit to be set in the SQF, then the bit is set even if the other detections did not have this condition. Sources with hot or dead pixels within 3 pixels of source center (bit 8), those in wings of saturated stars (bit 20), and those within 3 pixels of the frame edge (bit 30) are culled from the Catalog.

Table 5 gives the Source Quality Flag bits and origin of the flag (SSC or GLIMPSE pipeline). Each of the 5 bands has its own Source Quality Flag. For the cross-band confusion flag and the cross-band merge lumping flag, when the condition is met for one of the bands, the bit is set for all the source's bands.

The value of the SQF is $\sum 2^{(bit-1)}$. For example, a source with bits 1 and 4 set will have SQF = $2^0 + 2^3 = 9$. If the SQF is 0, the source has no detected problems. More information about these flags and a bit value key can be found in Appendix B.

Table 5. Source Quality Flag (SQF) Bits

SQF bit	Description	Origin
1	poor pixels in dark current	SSC pmask
2	flat field questionable	SSC dmask
3	latent image	SSC dmask
3	persistence (p)	2MASS
4	photometric confusion (c)	2MASS
8	hot, dead or otherwise unacceptable pixel	SSC pmask,dmask,GLIMPSE
9	electronic stripe (s)	2MASS
10	DAOPHOT tweak positive	GLIMPSE
11	DAOPHOT tweak negative	GLIMPSE
13	confusion in in-band merge	GLIMPSE
14	confusion in cross-band merge (IRAC)	GLIMPSE
14	confusion in cross-band merge (2MASS)	GLIMPSE
15	column pulldown corrected	GLIMPSE
19	data predicted to saturate	GLIMPSE
20	saturated star wing region	GLIMPSE
20	diffraction spike (d)	2MASS
21	pre-lumping in in-band merge	GLIMPSE
22	post-lumping in cross-band merge (IRAC)	GLIMPSE
22	post-lumping in cross-band merge (2MASS)	GLIMPSE
23	photometry quality flag	2MASS
24	photometry quality flag	2MASS
25	photometry quality flag	2MASS
30	within three pixels of edge of frame	GLIMPSE

• Flux calculation Method Flag (MF_i). The flux calculation method flag indicates by bit whether a given frametime was present, and whether that frametime was used in the final flux. Table 6 defines the values for this flag: value= $2^{(present\_bit-1)} + 2^{(used\_bit-1)}$

Table 6. Flux Calculation Method Flag (MF)

ft	present		used	
(sec)	bit	(value)	bit	(value)
0.6	1	(1)	2	(2)
1.2	3	(4)	4	(8)
2	5	(16)	6	(32)
12	7	(64)	8	(128)
30	9	(256)	10	(512)
100	11	(1024)	12	(2048)

For example, if 0.6 and 12 sec frametime data were present, but only the 12 sec data were used, then bits 1 and 7 will be set (fluxes present) and bit 8 will be set (12 sec used) and the MF will be $2^0 + 2^6 + 2^7 = 1 + 64 + 128 = 193$ (see Table 6). Note that, in practice, MF of 193 is rarely assigned because some detections are thrown out at the beginning of bandmerging because of sensitivity or saturation issues (§3.3).

For GLIMPSE360 12/0.6 sec frametime HDR mode, the relevant numbers work out to be

3 - short exp data used, long exp data absent
67 - short used, long present but unused
192 - long exp used, short absent
193 - long exp used, short present but unused

5.2 GLIMPSE360 Image Atlas

Using the Montage package, the IRAC images are mosaicked into rectangular tiles that cover the surveyed region. The units are MJy/sr and the coordinates are Galactic. The mosaic images conserve surface brightness in the original images. We provide 1.2″ pixel mosaics as well as higher resolution 0.6″ pixel mosaics. We provide larger (e.g. 3.1°×3.6°, 3.1°×3.8°, 3.1°×4.2°, and 3.1°×4.6°) FITS files with a pixel size of 1.2″ , with and without background matching and gradient correction, for an overview look that covers the full latitude range of the GLIMPSE360 areas. The background matching and gradient removal may be removing real sky variations so we provide these images *in addition* to the 1.2″ pixel images that do not have the background matching. The angular sizes of the higher resolution tiles (pixel size of 0.6″) are 1.1°×1.1°, 1.1°×1.2°and 1.1°×1.3°. Three tiles span the latitude range of the areas. World Coordinate System (WCS) keywords are standard (CTYPE, CRPIX, CRVAL, CD matrix keywords) with a Galactic projection (GLON-CAR, GLAT-CAR; Calabretta and Greisen 2002). See (§6.2) for an example of a FITS header. The mosaicked images are 32-bit IEEE floating point single-extension FITS formatted images. For a quick-look of the mosaics, we provide 3-color jpeg files (IRAC [3.6], [4.5] and WISE [12]) for each area covered by the FITS files. These are rebinned to much lower resolution to make the files small. Some artifacts remain in the images since removing them would cause gaps in coverage. Appendix C gives examples of some of the artifacts still found in the GLIMPSE360 images. Since the WISE [12] images have been included in our 3-color jpegs, Appendix C also gives examples of some of the more noticeable artifacts that appear in the WISE [12] images.

5.3 Web Infrared Tool Shed

The Web Infrared Tool Shed (WITS) (dustem.astro.umd.edu) contains two toolboxes: the Dust Infrared Toolbox (DIRT) and the PhotoDissociation Region Toolbox (PDRT). The toolboxes provide extensive databases of circumstellar shell emission models and PDR emission models. Users input data and retrieve best fit models. DIRT output includes central source and dust shell parameters. PDRT output consists of gas density, temperature, incident UV field and IR line intensities.

Legacy Tools include, for DIRT, a retrievable database of SEDs convolved with IRAC bands, an IRAC specific input GUI (Graphic User Interface), and an extended model base containing embedded high mass stars and low luminosity protostars with and without illumination by an external field. It also includes models with alternate grain models including ice mantles.

Spitzer enhancements to PDRT consist of PDR lines (Si II, Fe II, H_2) useful for Infrared Spectrograph (IRS) observations and interpretation of IRAC PDR emission.

DIRT is based on the radiation transfer code of Wolfire and Cassinelli (1986) that calculates the passage of stellar radiation through a spherical dust envelope. The web interface to DIRT is a JAVA applet which accesses a catalog of pre-run spectral energy distributions. There are currently about 400,000 models on-line. Users can display models with various properties including:

Table 7. Ranges of the DIRT Tool

Parameters	Current values	*Spitzer* enhancements
The gas density power law:	0, -0.5, -1.0, -1.5, -2.0	
Stellar Luminosity (L_0):	10,30,50,100,....5×10^5	1e-5,3e-5,5e-5,....1
Effective temperature (K):	3e3,5e3,1e4,3e4,4e4	1e3,1.5e3,2e3,2.5e3,3e3
Outer Shell Radius (cm):	1e14,3e14,5e14,....5e18	1e11,3e11,5e11....5e15
Inner Shell Radius (cm):	1e13 to Outer Radius/10	1e11 to Outer Radius/10
A_V through Shell:	1,3,5,10,....5e3	1,3,5,10,....5e2

The models are displayed in an interactive plot window showing flux versus frequency for a series of models with increasing A_V. Users can change scale, color code models, axes, etc. Users can input observations with error bars and beam sizes and run a χ^2 fit to find the best model. The best fit is overlayed with observations and error bars. Additional details are displayed including the run of gas density and gas temperature, the run of grain temperatures, emitted intensity across model source at various wavelengths, and flux versus beam size for a beam centered on the source at various wavelengths. Flux and source size are scaled to input distance. A *Spitzer* specific interface accepts IRAC and MIPS data input. Models are retrievable and displayed in IRAC band integrated quantities. Model space is searched for the best fit from the input IRAC observations. For each band, plots show model flux versus wavelength (μm) and model surface brightness versus source size ($''$).

PDRT is based on the photodissociation region code of Tielens and Hollenbach 1985 and updated by Wolfire, Tielens, and Hollenbach 1990, Kaufman et al. 1999, and Kaufman et al. 2006. The interface to PDRT allows users to input three or more spectral line observations, with errors, and χ^2 contour plots are generated showing the best fit model parameters to their data set. The output model parameters are the incident ultraviolet radiation field, the gas density, and the gas temperature. In addition, several predicted line intensities are given that match the best fit model. Current lines include the dominant coolants of PDRs including [C II] 158 μm, [O I] 63 μm, and

CO (J=1-0), plus several weaker lines that are also observable e.g., [O I] 145 μm, and [C I] 370 μm and 610 μm. Updates to the on-line models include [Si II] 35 μm and [Fe II] 26 μm, H_2 0-0S(0) 28.2 μm, 0-0S(1) 17.0 μm, and 0-0S(2) 12.3 μm, all observable by *Spitzer* IRS. Model results are given for local ISM abundances and for abundances a factor of 3 times higher. These emission lines along with IRAC maps of PDRs may be used to constrain the PDR properties including the distribution and abundance of polycyclic aromatic hydrocarbons (PAHs), as well as the efficiency of grain photoelectric heating.

5.4 YSO Grid and Fitter

To help interpret the many thousands of newly discovered Young Stellar Objects (YSOs) observed by the *Spitzer Space Telescope*, we have developed a tool to fit their Spectral Energy Distributions (SEDs) from a large grid of model SEDs produced by a 2-D radiation transfer code (Robitaille et al. 2006, 2007). Each model includes a central star that illuminates and heats a disk and a rotationally-flattened infalling envelope with bipolar cavities (Whitney et al. 2003a,b, 2004). Our grid includes a reasonably wide range of envelope and disk parameter values at each stellar age and mass to simulate a variety of evolutionary stages. For example, an early stage source is expected to have a high envelope infall rate and narrow bipolar cavities, whereas a later stage source may just have a disk without an envelope; but we allow for a large range of variation in each.

We have made the model YSO grid and SED fitting tool publicly available (caravan.astro.wisc.edu/protostars). Our website contains a browser that allows users to examine SEDs from each model for a range of viewing angles and apertures. Various components of each model SED can be viewed, including for example the flux originating from the central star, disk, or envelope, as shown in Figure 9. We have found the grid very useful for exploring how the SED of a YSO is affected by various parameters (e.g. Robitaille et al 2006). Also available on the website are files containing the fluxes in specific filters, e.g. IRAC or MIPS, for all models. Figure 9 shows how these files can be used to produce color-color plots for comparison to data.

Another main section on the website is an interface for our SED fitting tool. The fitting tool uses linear regression to quantify how well each model fits a given set of data. How well a parameter is constrained is determined directly from the range of parameter values for the well-fit SEDs. The online interface to this tool allows users to enter fluxes or magnitudes in specific filters (e.g. IRAC or MIPS), or fluxes at specific wavelengths (e.g. IRS fluxes). Figure 10 shows an example of fits to the SED of the T Tauri star AA Tau using fluxes specified in broadband filters; and to the SED of a massive embedded source, G10.62-0.38, including IRS data. Both figures were generated from the web server.

A new grid of models, including imaging is being produced. Feedback is appreciated, and can be made through a form on the website.

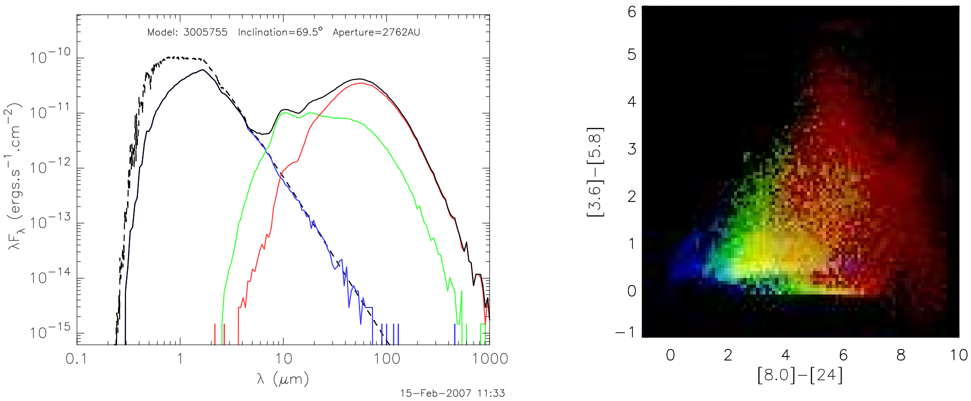

Figure 9: *Left:* A model SED downloaded from the grid browser. The lines show the total spectrum (black), the unextincted stellar atmosphere (dotted line), and flux that originated in the disk (green), envelope (red), and star (blue). *Right:* A color-color diagram produced from the model grid for a star formation region at a distance of 5 kpc. Three stages of evolution are shown in true-color (red: embedded stage, green: optically thick disk stage, blue: optically thin disk). The colors blend in regions occupied by multiple evolutionary stages.

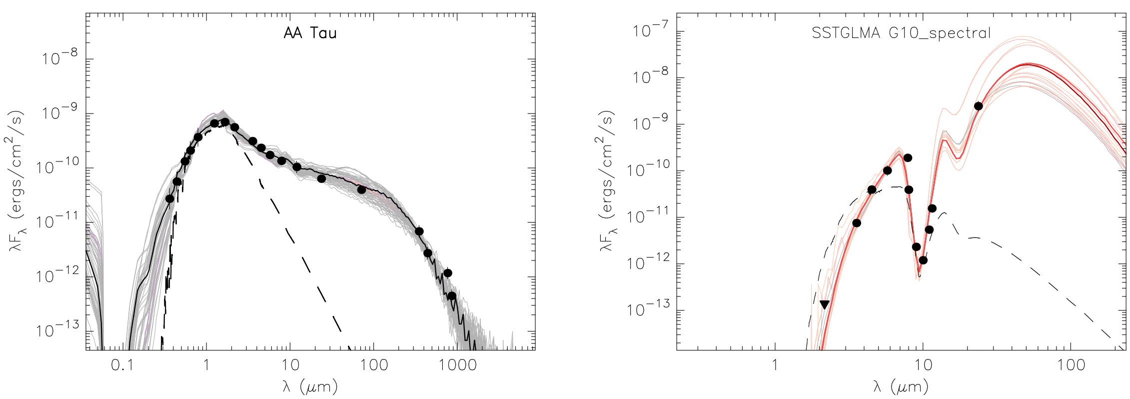

Figure 10: *Left:* Model SED fits (grey lines) to broadband photometry of AA Tau. *Right:* Model fits (colors indicate different apertures) to broadband photometry and a few IRS points for G10.62-0.38. The dashed line shows the extincted input stellar atmosphere.

6 Product Formats

6.1 Catalog and Archive

• The Catalog and Archive are broken into 4° (longitude) x 3° (latitude) areas for the GLIMPSE360 Survey. The Catalog and Archive files are in IPAC Table Format. Filenames are GLM360C_llmin-lmax.tbl and GLM360A_llmin-lmax.tbl, for the Catalog and Archive respectively (e.g. GLM360C_l133-137.tbl, GLM360C_l137-140.tbl, GLM360A_l133-137.tbl, GLM360A_l137-140.tbl, etc.) The entries are sorted by increasing Galactic longitude within each file.

An example of a GLM360C entry is

SSTGLMC G134.8079+01.5800 02352971+6201420 1200475009 134.807966 1.580017 0.3 0.3
38.873822 62.028340 0.3 0.3 0 15.788 0.068 15.403 0.116 15.144 0.146
14.979 0.059 14.938 0.048 99.999 99.999 99.999 99.999
7.714E-01 4.831E-02 7.065E-01 7.548E-02 5.839E-01 7.852E-02
2.865E-01 1.545E-02 1.902E-01 8.431E-03 -9.999E+02 -9.999E+02 -9.999E+02 -9.999E+02
1.191E-02 7.938E-03 -9.999E+02 -9.999E+02 1.580E-01 1.180E-01 -9.999E+02 -9.999E+02
15.97 9.36 7.44 18.54 22.56 -9.99 -9.99 48.4 28.8 -9.9 -9.9
3 6 0 0 3 6 0 0 29360128 25165824 25165824 1536 17408 -9 -9 192 192 -9 -9

Table 8 gives all of the available fields per source. Table 9 shows how to decode the above entry into these fields. All fields associated with IRAC bands [5.8] and [8.0] have been nulled for the Warm Mission GLIMPSE360 survey.

- Each source in both the Catalog and Archive has the entries given below.

Table 8. Fields in the Catalog and Archive

Column	Name	Description	Units	Data Type	Format	Nulls OK? or Value
1	designation	Catalog (SSTGLMC GLLL.llll±BB.bbbb) Archive (SSTGLMA GLLL.llll±BB.bbbb)	-	ASCII	A26	No
2	tmass_desig	2MASS PSC designation	-	ASCII	A16	null
3	tmass_cntr	2MASS counter (unique identification number)	-	I*4	I10	0
4	l	Galactic longitude	deg	R*8	F11.6	No
5	b	Galactic latitude	deg	R*8	F11.6	No
6	dl	Uncertainty in Gal. longitude	arcsec	R*8	F7.1	No
7	db	Uncertainty in Gal. latitude	arcsec	R*8	F7.1	No
8	ra	Right ascension (J2000)	deg	R*8	F11.6	No
9	dec	Declination (J2000)	deg	R*8	F11.6	No
10	dra	Uncertainty in right ascension	arcsec	R*8	F7.1	No
11	ddec	Uncertainty in declination	arcsec	R*8	F7.1	No
12	csf	Close source flag	-	I*2	I4	No
13–18	mag_t,dmag_t	Magnitudes & 1σ uncertainty in t=J,H,K_s bands	mag	R*4	6F7.3	99.999,99.999
19–26	mag_i,dmag_i	Magnitudes & 1σ uncertainty in IRAC band i	mag	R*4	8F7.3	99.999,99.999
27–32	F_t,dF_t	Fluxes & 1σ uncertainty in t=J,H,K_s bands	mJy	R*4	6E11.3	-999.9,-999.9
33–40	F_i,dF_i	Fluxes & 1σ uncertainty in IRAC band i	mJy	R*4	8E11.3	-999.9,-999.9
41–44	F_i_rms	RMS dev. of individual detections from F_i	mJy	R*4	4E11.3	-999.9
45–48	sky_i	Local sky bkg. for IRAC band i flux	MJy/sr	R*4	4E11.3	-999.9
49–51	SN_t	Signal/Noise for bands t=J,H,K_s	-	R*4	3F7.2	-9.99
52–55	SN_i	Signal/Noise for IRAC band i flux	-	R*4	4F7.2	-9.99
56–59	$\mathrm{srcdens}_i$	Local source density for IRAC band i object	no./sq $'$	R*4	4F9.1	-9.9
60–63	M_i	Number of detections for IRAC band i	-	I*2	4I6	No
64–67	N_i	Number of possible detections for IRAC band i	-	I*2	4I6	No
68–70	SQF_t	Source Quality Flag for t=J,H,K_s flux	-	I*4	3I11	-9
71–74	SQF_i	Source Quality Flag for IRAC band i flux	-	I*4	4I11	-9
75–78	MF_i	Flux calc method flag for IRAC band i flux	-	I*2	4I6	-9

Table 9. Example of Catalog/Archive Entry

designation	SSTGLMC G134.8079+01.5800	Name
tmass_desig	02352971+6201420	2MASS designation
tmass_cntr	1200475009	2MASS counter
l,b	134.807966 1.580017	Galactic Coordinates (deg)
dl,db	0.3 0.3	Uncertainty in Gal. Coordinates (arcsec)
ra,dec	38.873822 62.028340	RA and Dec (J2000.0) (deg)
dra,ddec	0.3 0.3	Uncertainty in RA and Dec (arcsec)
csf	0	Close source flag
mag,dmag	15.788 15.403 15.144	Magnitudes (2MASS J,H,K_s) (mag)
	0.068 0.116 0.146	Uncertainties (2MASS) (mag)
mag,dmag	14.979 14.938 99.999 99.999	Magnitudes (IRAC 3.6,4.5,5.8,8.0 μm) (mag)
	0.059 0.048 99.999 99.999	Uncertainties (IRAC) (mag)
F,dF	7.714E-01 7.065E-01 5.839E-01	2MASS Fluxes (mJy)
	4.831E-02 7.548E-02 7.852E-02	Uncertainties in 2MASS fluxes (mJy)
F,dF	2.865E-01 1.902E-01 -9.999E+02 -9.999E+02	IRAC Fluxes (mJy)
	1.545E-02 8.431E-03 -9.999E+02 -9.999E+02	Uncertainties in IRAC fluxes (mJy)
F_rms	1.191E-02 7.938E-03 -9.999E+02 -9.999E+02	RMS_flux (mJy) (IRAC)
sky	1.580E-01 1.180E-01 -9.999E+02 -9.999E+02	Sky Bkg (MJy/sr) (IRAC)
SN	15.97 9.36 7.44	Signal to Noise (2MASS)
SN	18.54 22.56 -9.99 -9.99	Signal to Noise (IRAC)
srcdens	48.4 28.8 -9.9 -9.9	Local Source Density (IRAC) (#/sq arcmin)
M	3 6 0 0	Number of detections (IRAC)
N	3 6 0 0	Number of possible detections (IRAC)
SQF	29360128 25165824 25165824	Source Quality Flag (2MASS)
SQF	1536 17408 -9 -9	Source Quality Flag (IRAC)
MF	192 192 -9 -9	Flux Calculation Method Flag (IRAC)

6.2 GLIMPSE360 Image Atlas

The mosaicked images for each IRAC band are standard 32-bit IEEE floating point single-extension FITS files in Galactic coordinates. Pixels that have no flux estimate have the value NaN. The FITS headers contain relevant information from both the SSC pipeline processing and the GLIMPSE processing such as IRAC frames included in the mosaicked image and coordinate information.

We provide native resolution images (1.2″ pixels) (e.g. 3.1°x 3.6° mosaic FITS files) for each band, along with low resolution 3-color jpegs. Other mosaics are 3.1°×3.8°, 3.1°×4.2°and 3.1°×4.6°. Filenames are GLM_*lcbc*_mosaic_I*ch*.fits, where *lc* and *bc* are the Galactic longitude and latitude of the center of the mosaic image, I denotes IRAC, and *ch* is the IRAC instrument channel number (1=[3.6] and 2=[4.5]). For example, GLM_13500+0095_mosaic_I1.fits is a 3.1°x 3.6° IRAC channel 1 [3.6] mosaic centered on l=135.00°, b=+0.95°. We provide low-resolution 3-color jpeg images for each area, combining IRAC [3.6] and [4.5] and WISE [12] to be used for quick-look purposes. The filename for this jpeg file is similar to the mosaic FITS file: e.g. GLM_13500+0095_3.1x3.6.jpg. We also provide the background matched and gradient corrected 1.2″ pixel mosaics and 3-color jpegs. The background matched and gradient corrected image filenames have "corr_" pre-pended to the filename (e.g. corr_GLM_13500+0095_mosaic_I1.fits). This comment line is added to the FITS header for these images:

```
COMMENT Background Matched, Gradient Corrected
```

The angular sizes of the higher resolution (0.6″ pixels) tiles are 1.1°×1.1°, 1.1°×1.2°and 1.1°×1.3°. Three tiles span the latitude range of the areas. There are three mosaics per 1.1 degree Galactic longitude interval with 0.05° overlap between mosaics. The filenames are similar to the other FITS and jpeg images: e.g. GLM_20750+0055_mosaic_I1.fits, GLM_20750+0055.jpg.

Here is an example of the FITS header for the 3.1°x 3.6° GLM_13500+0095_mosaic_I1.fits:

```
SIMPLE  =                    T / file does conform to FITS standard
BITPIX  =                  -32 / number of bits per data pixel
NAXIS   =                    2 / number of data axes
NAXIS1  =                 9300 / length of data axis 1
NAXIS2  =                10800 / length of data axis 2
COMMENT   FITS (Flexible Image Transport System) format is defined in 'Astronomy
COMMENT   and Astrophysics', volume 376, page 359; bibcode: 2001A&A...376..359H
TELESCOP= 'SPITZER '           / Telescope
INSTRUME= 'IRAC    '           / Instrument ID
ORIGIN  = 'UW Astronomy Dept'  / Installation where FITS file written
CREATOR = 'GLIMPSE Pipeline'   / SW that created this FITS file
CREATOR1= 'S18.18.0'           / SSC pipeline that created the BCD
PIPEVERS= '1v04    '           / GLIMPSE pipeline version
MOSAICER= 'Montage V3.0'       / SW that originally created the Mosaic Image
FILENAME= 'GLM_13500+0095_mosaic_I1.fits' / Name of associated fits file
PROJECT = 'FGL360L '           / Project ID
FILETYPE= 'mosaic  '           / Calibrated image(mosaic)/residual image(resid)
CHNLNUM =                    1 / 1 digit Instrument Channel Number
DATE    = '2011-05-14T06:26:42' / file creation date (YYYY-MM-DDThh:mm:ss UTC)
COMMENT --------------------
COMMENT Proposal Information
COMMENT --------------------
OBSRVR  = 'Barbara Whitney'    / Observer Name
OBSRVRID=                31113 / Observer ID of Principal Investigator
PROCYCLE=                    9 / Proposal Cycle
PROGID  =                60020 / Program ID
PROTITLE= 'GLIMPSE360: Completing the Spi' / Program Title
PROGCAT =                   30 / Program Category
COMMENT -----------------------------
COMMENT Time and Exposure Information
COMMENT -----------------------------
SAMPTIME=                  0.2 / [sec] Sample integration time
FRAMTIME=                 12.0 / [sec] Time spent integrating each BCD frame
EXPTIME =                 10.4 / [sec] Effective integration time each BCD frame
COMMENT DN per pixel=flux(photons/sec/pixel)/gain*EXPTIME
NEXPOSUR=                    3 / Typical number of exposures
COMMENT Total integration time for the mosaic = EXPTIME * NEXPOSUR
COMMENT Total DN per pixel=flux(photons/sec/pixel)/gain*EXPTIME*NEXPOSUR
AFOWLNUM=                    8 / Fowler number
COMMENT --------------------
COMMENT Pointing Information
COMMENT --------------------
CRPIX1  =            4650.5000 / Reference pixel for x-position
CRPIX2  =            5400.5000 / Reference pixel for y-position
CTYPE1  = 'GLON-CAR'           / Projection Type
```

```
CTYPE2  = 'GLAT-CAR'           / Projection Type
CRVAL1  =        135.00000000 / [Deg] Galactic Longtitude at reference pixel
CRVAL2  =          0.94999999 / [Deg] Galactic Latitude at reference pixel
EQUINOX =              2000.0 / Equinox for celestial coordinate system
DELTA-X =          3.09999990 / [Deg] size of image in axis 1
DELTA-Y =          3.59999990 / [Deg] size of image in axis 2
BORDER  =          0.00000000 / [Deg] mosaic grid border
CD1_1   =     -3.33333330E-04
CD1_2   =      0.00000000E+00
CD2_1   =      0.00000000E+00
CD2_2   =      3.33333330E-04
PIXSCAL1=               1.200 / [arcsec/pixel] pixel scale for axis 1
PIXSCAL2=               1.200 / [arcsec/pixel] pixel scale for axis 2
OLDPIXSC=               1.221 / [arcsec/pixel] pixel scale of single IRAC frame
RA      =         38.72928619 / [Deg] Right ascension at mosaic center
DEC     =         61.37329483 / [Deg] Declination at mosaic center
COMMENT ----------------------
COMMENT Photometry Information
COMMENT ----------------------
BUNIT   = 'MJy/sr  '           / Units of image data
GAIN    =                 3.7 / e/DN conversion
JY2DN   =         2368651.500 / Average Jy to DN Conversion
ETIMEAVE=             10.4000 / [sec] Average exposure time for the BCD frames
PA_AVE  =               84.86 / [deg] Average position angle
ZODY_EST=             0.05564 / [Mjy/sr] Average ZODY_EST
ZODY_AVE=             0.01378 / [Mjy/sr] Average ZODY_EST-SKYDRKZB
COMMENT Flux conversion (FLUXCONV) for this mosaic =
COMMENT Average of FLXC from each frame*(old pixel scale/new pixel scale)**2
FLUXCONV=         0.129723862 / Average MJy/sr to DN/s Conversion
COMMENT ----------------------------
COMMENT AORKEYS/ADS Ident Information
COMMENT ----------------------------
AOR001  = '0038758656'         / AORKEYS used in this mosaic
AOR002  = '0038787072'         / AORKEYS used in this mosaic
AOR003  = '0038763776'         / AORKEYS used in this mosaic
AOR004  = '0038784512'         / AORKEYS used in this mosaic
AOR005  = '0038763520'         / AORKEYS used in this mosaic
AOR006  = '0038792704'         / AORKEYS used in this mosaic
AOR007  = '0038753280'         / AORKEYS used in this mosaic
AOR008  = '0038759936'         / AORKEYS used in this mosaic
AOR009  = '0038759424'         / AORKEYS used in this mosaic
AOR010  = '0038766592'         / AORKEYS used in this mosaic
AOR011  = '0038798592'         / AORKEYS used in this mosaic
AOR012  = '0038798080'         / AORKEYS used in this mosaic
AOR013  = '0038752768'         / AORKEYS used in this mosaic
AOR014  = '0038755840'         / AORKEYS used in this mosaic
AOR015  = '0038784768'         / AORKEYS used in this mosaic
AOR016  = '0038801408'         / AORKEYS used in this mosaic
```

```
AOR017  = '0038763264'         / AORKEYS used in this mosaic
AOR018  = '0038790400'         / AORKEYS used in this mosaic
AOR019  = '0038749952'         / AORKEYS used in this mosaic
AOR020  = '0038782208'         / AORKEYS used in this mosaic
AOR021  = '0038799360'         / AORKEYS used in this mosaic
AOR022  = '0038746368'         / AORKEYS used in this mosaic
AOR023  = '0038790656'         / AORKEYS used in this mosaic
AOR024  = '0038745344'         / AORKEYS used in this mosaic
AOR025  = '0038798848'         / AORKEYS used in this mosaic
AOR026  = '0038782976'         / AORKEYS used in this mosaic
AOR027  = '0038797824'         / AORKEYS used in this mosaic
AOR028  = '0038776832'         / AORKEYS used in this mosaic
AOR029  = '0038769408'         / AORKEYS used in this mosaic
AOR030  = '0038744064'         / AORKEYS used in this mosaic
AOR031  = '0038748928'         / AORKEYS used in this mosaic
AOR032  = '0038770944'         / AORKEYS used in this mosaic
AOR033  = '0038802688'         / AORKEYS used in this mosaic
AOR034  = '0038776064'         / AORKEYS used in this mosaic
AOR035  = '0038756608'         / AORKEYS used in this mosaic
AOR036  = '0038779904'         / AORKEYS used in this mosaic
AOR037  = '0038799104'         / AORKEYS used in this mosaic
AOR038  = '0038780672'         / AORKEYS used in this mosaic
AOR039  = '0038744832'         / AORKEYS used in this mosaic
AOR040  = '0038746112'         / AORKEYS used in this mosaic
AOR041  = '0038747648'         / AORKEYS used in this mosaic
AOR042  = '0038757632'         / AORKEYS used in this mosaic
AOR043  = '0038785792'         / AORKEYS used in this mosaic
DSID001 = 'ads/sa.spitzer#0038758656' / Data Set Identification for ADS/journals
DSID002 = 'ads/sa.spitzer#0038787072' / Data Set Identification for ADS/journals
DSID003 = 'ads/sa.spitzer#0038763776' / Data Set Identification for ADS/journals
DSID004 = 'ads/sa.spitzer#0038784512' / Data Set Identification for ADS/journals
DSID005 = 'ads/sa.spitzer#0038763520' / Data Set Identification for ADS/journals
DSID006 = 'ads/sa.spitzer#0038792704' / Data Set Identification for ADS/journals
DSID007 = 'ads/sa.spitzer#0038753280' / Data Set Identification for ADS/journals
DSID008 = 'ads/sa.spitzer#0038759936' / Data Set Identification for ADS/journals
DSID009 = 'ads/sa.spitzer#0038759424' / Data Set Identification for ADS/journals
DSID010 = 'ads/sa.spitzer#0038766592' / Data Set Identification for ADS/journals
DSID011 = 'ads/sa.spitzer#0038798592' / Data Set Identification for ADS/journals
DSID012 = 'ads/sa.spitzer#0038798080' / Data Set Identification for ADS/journals
DSID013 = 'ads/sa.spitzer#0038752768' / Data Set Identification for ADS/journals
DSID014 = 'ads/sa.spitzer#0038755840' / Data Set Identification for ADS/journals
DSID015 = 'ads/sa.spitzer#0038784768' / Data Set Identification for ADS/journals
DSID016 = 'ads/sa.spitzer#0038801408' / Data Set Identification for ADS/journals
DSID017 = 'ads/sa.spitzer#0038763264' / Data Set Identification for ADS/journals
DSID018 = 'ads/sa.spitzer#0038790400' / Data Set Identification for ADS/journals
DSID019 = 'ads/sa.spitzer#0038749952' / Data Set Identification for ADS/journals
DSID020 = 'ads/sa.spitzer#0038782208' / Data Set Identification for ADS/journals
DSID021 = 'ads/sa.spitzer#0038799360' / Data Set Identification for ADS/journals
```

```
DSID022 = 'ads/sa.spitzer#0038746368' / Data Set Identification for ADS/journals
DSID023 = 'ads/sa.spitzer#0038790656' / Data Set Identification for ADS/journals
DSID024 = 'ads/sa.spitzer#0038745344' / Data Set Identification for ADS/journals
DSID025 = 'ads/sa.spitzer#0038798848' / Data Set Identification for ADS/journals
DSID026 = 'ads/sa.spitzer#0038782976' / Data Set Identification for ADS/journals
DSID027 = 'ads/sa.spitzer#0038797824' / Data Set Identification for ADS/journals
DSID028 = 'ads/sa.spitzer#0038776832' / Data Set Identification for ADS/journals
DSID029 = 'ads/sa.spitzer#0038769408' / Data Set Identification for ADS/journals
DSID030 = 'ads/sa.spitzer#0038744064' / Data Set Identification for ADS/journals
DSID031 = 'ads/sa.spitzer#0038748928' / Data Set Identification for ADS/journals
DSID032 = 'ads/sa.spitzer#0038770944' / Data Set Identification for ADS/journals
DSID033 = 'ads/sa.spitzer#0038802688' / Data Set Identification for ADS/journals
DSID034 = 'ads/sa.spitzer#0038776064' / Data Set Identification for ADS/journals
DSID035 = 'ads/sa.spitzer#0038756608' / Data Set Identification for ADS/journals
DSID036 = 'ads/sa.spitzer#0038779904' / Data Set Identification for ADS/journals
DSID037 = 'ads/sa.spitzer#0038799104' / Data Set Identification for ADS/journals
DSID038 = 'ads/sa.spitzer#0038780672' / Data Set Identification for ADS/journals
DSID039 = 'ads/sa.spitzer#0038744832' / Data Set Identification for ADS/journals
DSID040 = 'ads/sa.spitzer#0038746112' / Data Set Identification for ADS/journals
DSID041 = 'ads/sa.spitzer#0038747648' / Data Set Identification for ADS/journals
DSID042 = 'ads/sa.spitzer#0038757632' / Data Set Identification for ADS/journals
DSID043 = 'ads/sa.spitzer#0038785792' / Data Set Identification for ADS/journals
NIMAGES =                 4318 / Number of IRAC Frames in Mosaic
```

In addition to the FITS header information given above, the associated ASCII .hdr file includes information about each IRAC frame used in the mosaic image. For example, GLM_13500+0095_mosaic_I1.hdr includes:

```
COMMENT ----------------------------------------
COMMENT Info on Individual Frames in Mosaic
COMMENT ----------------------------------------
IRFR0001= 'SPITZER_I1_0038758656_0063_0000_02_levbflx.fits' / IRAC frame
DOBS0001= '2010-03-13T05:21:56.835' / Date & time at frame start
MOBS0001=      55268.222656250 / MJD (days) at frame start
RACE0001=            34.990429 / [Deg] Right ascension at reference pixel
DECC0001=            60.817371 / [Deg] Declination at reference pixel
PANG0001=                80.40 / [deg] Position angle for this image
FLXC0001=              0.12530 / Flux conversion for this image
ZODE0001=              0.05722 / [MJy/sr] ZODY_EST for this image
ZODY0001=              0.01515 / [MJy/sr] ZODY_EST-SKYDRKZB for this image
IRFR0002= 'SPITZER_I1_0038758656_0087_0000_02_levbflx.fits' / IRAC frame
DOBS0002= '2010-03-13T05:27:01.230' / Date & time at frame start
MOBS0002=      55268.226562500 / MJD (days) at frame start
RACE0002=            34.835697 / [Deg] Right ascension at reference pixel
DECC0002=            60.776794 / [Deg] Declination at reference pixel
```

```
PANG0002=                80.26 / [deg] Position angle for this image
FLXC0002=              0.12530 / Flux conversion for this image
ZODE0002=              0.05726 / [MJy/sr] ZODY_EST for this image
ZODY0002=              0.01519 / [MJy/sr] ZODY_EST-SKYDRKZB for this image
.
.       Information on the IRAC frame: filename, date of observation, central
.       position, position angle, flux convert and zodiacal light for
.       frames 3 through 4316
.
IRFR4317= 'SPITZER_I1_0038799360_0157_0000_02_levbflx.fits' / IRAC frame
DOBS4317= '2010-03-14T05:00:26.412' / Date & time at frame start
MOBS4317=      55269.207031250 / MJD (days) at frame start
RACE4317=            40.181694 / [Deg] Right ascension at reference pixel
DECC4317=            60.442623 / [Deg] Declination at reference pixel
PANG4317=                83.73 / [deg] Position angle for this image
FLXC4317=              0.12530 / Flux conversion for this image
ZODE4317=              0.05739 / [MJy/sr] ZODY_EST for this image
ZODY4317=              0.01533 / [MJy/sr] ZODY_EST-SKYDRKZB for this image
IRFR4318= 'SPITZER_I1_0038799360_0003_0000_02_levbflx.fits' / IRAC frame
DOBS4318= '2010-03-14T04:27:48.633' / Date & time at frame start
MOBS4318=      55269.187500000 / MJD (days) at frame start
RACE4318=            40.503521 / [Deg] Right ascension at reference pixel
DECC4318=            60.487461 / [Deg] Declination at reference pixel
PANG4318=                84.01 / [deg] Position angle for this image
FLXC4318=              0.12530 / Flux conversion for this image
ZODE4318=              0.05735 / [MJy/sr] ZODY_EST for this image
ZODY4318=              0.01528 / [MJy/sr] ZODY_EST-SKYDRKZB for this image
```

6.3 Web Infrared Tool Shed

The output from PDRT is in the form of contour plots in FITS, postscript, or GIF format. Pre-generated diagnostic plots as well as plots with observation overlays can be downloaded directly from the web interface. The model output from DIRT can be downloaded as ASCII tables directly from the web interface.

6.4 YSO Grid and Fitter

Models from the YSO grid are available as ASCII SEDs and postscript plots. In addition, the ASCII input files are available for each model, if the user wishes to run our publicly available radiation transfer code. Fitter fluxes from all the models are available in ASCII format. Results from the SED fitter are in the form of postscript files.

7 APPENDIX A - Flux Calibration Issues for Data Taken during the Cold to Warm Transition

Some of the GLIMPSE360 data were taken in the transition period from the Cold to Warm Spitzer Mission. On May 15, 2009 Spitzer used the last of its cryogen. The telescope and instrument slowly warmed to their new temperature. Data taken between May 15 and September 18, 2009 are affected by the fact that the temperature had not stabilized yet. See Sections 1 and 3 of the Spitzer IRAC Warm Features and Caveats document (irsa.ipac.caltech.edu/data/SPITZER/docs/irac/warmfeatures/) for more details about the calibration issues.

Most of the GLIMPSE360 data taken from l=89.7°-102.5° were observed during this time of transition. The GLIMPSE360 data taken in the IRACPC03 campaign were taken from September 3-9, 2009 and the GLIMPSE360 data taken in the IRACPC04 campaign were taken from September 10-15, 2009. Figure 11 shows the areas covered in the PC03 and PC04 campaigns, overlayed on the [3.6] GLIMPSE360 image. The PC03 data were processed by SSC pipeline S18.12.0 and the PC04 data were processed by version S18.18.0.

The program "Spitzer Mapping of the Outer Galaxy" (SMOG; PI Sean Carey; PID=50398) mapped a 21 square degree area from l=102°to 109°and b=0°to 3°. We have processed these data with our pipeline. We compared the GLIMPSE360 fluxes from the PC04 campaign (there was no overlap with SMOG in the PC03 data) with the SMOG fluxes for the same sources at the l=102° boundary between the two projects. For the PC04 data that overlap the SMOG data the following offsets between the GLIMPSE360 and SMOG fluxes are observed:

```
band      area of overlap    PC04-SMOG mean offset (mag)
[3.6]    l=101.68  b=+2.48       0.068
[4.5]    l=101.70  b=+2.55       0.031
```

There are small areas of overlap between GLIMPSE360 and SMOG where the PC04 data are mixed with GLIMPSE360 data that were taken later and thus should not be affected by the temperature instability and resulting calibration issue. In these areas the offsets are slightly less:

```
band      area of overlap    PC04mix-SMOG mean offset (mag)
[3.6]    l=102.10  b=+1.03       0.041
[4.5]    l=102.09  b=+1.72       0.027
```

For the PC03 data, where there is no overlap with SMOG, we compared fluxes on the l=90° end. We compared the PC04 fluxes with the GLIMPSE360 data taken much later (July 2010). Single frame comparisons were made between the two datasets and we found

```
band      area of overlap    PC03-GLM360 mean offset (mag)
[3.6]    l=090.21  b=+2.71       0.052
[4.5]    l=090.21  b=+2.73       0.000
```

We also compared the fluxes of two areas of overlap between SMOG and GLIMPSE360 at the l=109° boundary. The GLIMPSE360 data were taken later (January 29-Febuary 3, 2010) and are unaffected by the temperature issue. The agreement between the two datasets is good and consistent.

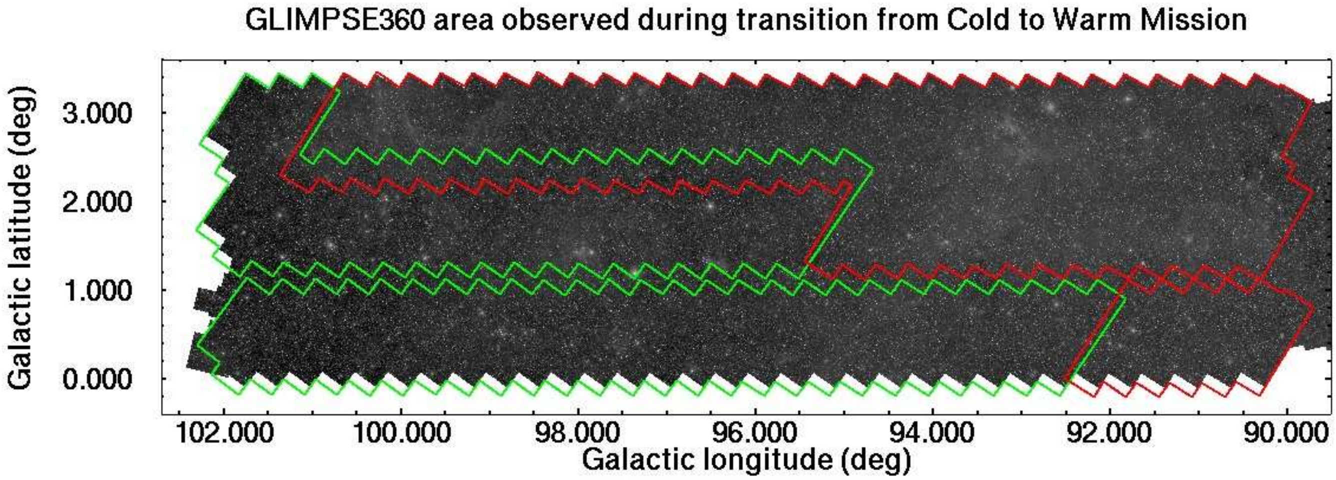

Figure 11: This figure shows the GLIMPSE360 area ([3.6] image shown) observed during the Cold to Warm Mission transition. The area enclosed in red is the PC03 campaign data. This data was taken September 3 to 9, 2009. The area enclosed in green is the PC04 data, observed September 10 to 15, 2009. There is a small amount of data around b=+1.2° that was taken at a later time.

```
Settled warmed-up SPITZER data
band       area of overlap    GLM360-SMOG mean offset (mag)
[3.6]     l=108.95  b=+1.41         0.012
[4.5]     l=108.95  b=+1.48         0.001

[3.6]     l=109.37  b=+0.76         0.012
[4.5]     l=109.36  b=+0.84        -0.001
```

In conclusion, if one is using GLIMPSE360 source lists in the l=89.7°to 102.5°area, most of the fluxes are affected by the fact that the tempertaure had not yet stabilized. The [3.6] fluxes will likely be about 0.07 magnitudes too faint and the [4.5] fluxes about 0.03 magnitudes too faint.

8 APPENDIX B - Source Quality Flag Bit Descriptions

A.1 IRAC Source Quality Flag

Information is gathered from the SSC IRAC bad pixel mask (pmask), SSC bad data mask (dmask) and the GLIMPSE IRAC pipeline for the Source Quality Flag. Table 5 lists the bits and the origin of the flag (SSC or GLIMPSE pipeline). See ssc.spitzer.caltech.edu/irac/products/pmask.html and ssc.spitzer.caltech.edu/irac/products/bcd_dmask.html for more information about the IRAC pmask and dmask.

bit
1 poor pixels in dark current

This bit is set when a source is within 3 pixels of a pixel identified in the SSC IRAC pmask as having poor dark current response (bits 7 and 10 in the pmask).

2 flat field questionable
If a pixel is flagged in the SSC IRAC dmask as flat field applied using questionable value (bit 7) or flat field could not be applied (bit 8), a source within 3 pixels of these pixels will have this bit set.

3 latent image
This flag comes from the latent image flag (bit 5) from the dmask. The SSC pipeline predicts the positions of possible latent images due to previously observed bright sources.

8 hot, dead or otherwise unacceptable pixel
Hot, dead or unacceptable pixels are identified in the IRAC pmask as having an unacceptable response to light (bits 8, 9 and 14 in the IRAC pmask). Also considered bad pixels are ones flagged as bad or missing in bit 11 and 14 in the IRAC dmask. SQF bit 8 is set if a source is within 3 pixels of any of these bad pixels. Sources with this bit set are culled from the Catalog.

10 DAOPHOT tweak positive
11 DAOPHOT tweak negative
Bits 10 and 11 correspond to an iterative photometric step (tweaking). Photometry is initially performed by DAOPHOT/ALLSTAR using PSF fitting. This photometric step produces a list of sources, their positions and brightnesses, as well as a residual image of those sources removed from the input image. By flattening the residual image (smoothing it and then subtracting the smoothed image from the residual image) and then performing small aperture photometry at the location of each of the extracted sources, it is possible to determine if the extracted source was over or under subtracted due to any local complex variable background or the undersampled PSF. SQF bit 10 refers to sources that were initially under-subtracted. From the aperture photometry a positive flux correction was applied to the DAOPHOT/ALLSTAR extraction value (source was brightened via aperture photometry as compared to the initial PSF fitted DAOPHOT/ALLSTAR photometry). SQF bit 11 refers to sources that were initially over-subtracted. Using aperture photometry, a negative flux correction was applied to the DAOPHOT/ALLSTAR extraction value (source was dimmed via aperture photometry as compared to the initial PSF fitted DAOPHOT/ALLSTAR photometry). Sources with both SQF bits 10 and 11 set imply 1) the source was initially under-subtracted, but the aperture photometry over- corrected and thus a second aperture correction was applied or 2) multiple observations in a band consisting of at least one observation with a positive tweak and another observation with a negative tweak.

13 confusion in in-band merge
14 confusion in cross-band merge
These bits are set during the bandmerging process. The bandmerger reports, for each source and band, the number of merge candidates it considered in each of the other bands. If the number of candidates is greater than 2, then the bandmerger had to resolve the choice based on examination of the different band-pair combinations and position (and flux in-band) χ^2 differences between candidates. If the number of candidates is greater than 1, the confusion flag is set.

15 column pulldown corrected ([3.6] and [4.5] bands)
This bit is set if the source is within 3 pixels of a column pulldown corrected pixel.

19 data predicted to saturate
This bit is set when a source is within 3 pixels of a pixel identified in the SSC IRAC dmask as being saturated (bit 10 in the dmask). GLIMPSE runs a saturated pixel predicter and sets bit 10 in the dmask. This program finds clusters of high-valued pixels. The cluster size and high pixel

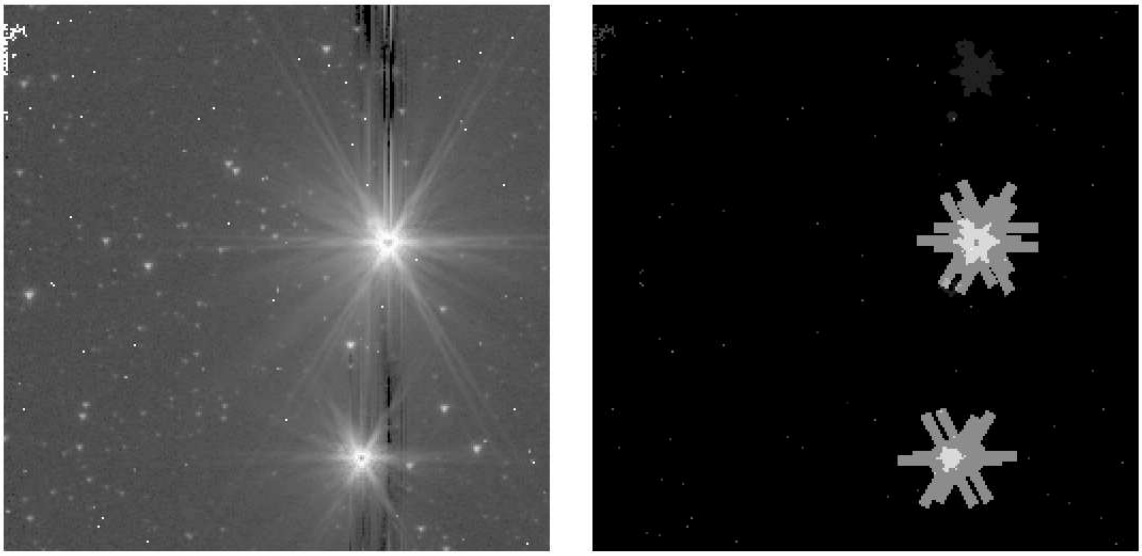

Figure 12: The [3.6] GLIMPSE360 IRAC frame (AOR 32845568, exposure 141) is on the left; the flags for that frame are shown on the right. The PSF-shaped areas around the bright sources correspond to SQF bit 20. Latent images are flagged at the top of the image, above the bright source. Various small dots are hot, dead or bad pixels (SQF bit 8). Bits in the SQF will have been set for sources within 3 pixels of any of the bad pixels.

value are tuned so that sources above the IRAC saturation limits are flagged as saturated. Before photometry is done on an IRAC frame, these pixels are masked.

20 saturated star wing region
False sources can be extracted in the wings of saturated sources. This bit is set if the source is within a PSF-shaped region (with a 24-pixel radius) surrounding a saturated source determined from bit 10 in the dmask. See Figure 12 for an example of the shapes of the saturated star wing areas flagged by this bit. Sources with this bit set are culled from the Catalog.

21 pre-lumping in in-band merge
Sources in the same IRAC frame within a radius of 1.6″ are merged into one source (weighted mean position and flux) before bandmerging. This is potentially a case in which the source is incompletely extracted in one IRAC frame and a second source extracted on another IRAC frame. Or it could be a marginally resolvable double source. This bit is set for the band if sources have been lumped for that band.

22 post-lumping in cross-band merge
This bit is set if the source is a result of sources that were lumped in the cross-band merge step. Cross-band lumping is done with a 1.6″ radius. For example, say there are two sources within 1.6″ of each other. One source has data in bands K_s and [3.6] and the other has data in band [4.5]. These two sources will be lumped into one source with data in two IRAC bands.

30 within three pixels of edge of frame
Sources within three pixels of the edge of the IRAC frame are flagged since it is likely to be too close to the edge of the frame for accurate photometry to be done. Sources with this bit set are culled from the Catalog.

A.2 2MASS Source Quality Flag

For the 2MASS bands, the following contamination and confusion (cc) flags from the 2MASS All-Sky Point Source Catalog are mapped into bits 3, 4, 9 and 20 of the source quality flag. For more information about the cc flags, see www.ipac.caltech.edu/2mass/releases/allsky/doc/sec2_2a.html#cc_flag. Users should consult the 2MASS PSC documentation for the complete information about the source, including all of their source quality flags.

bit

3 "p" persistence
Source may be contaminated by a latent image left by a nearby bright star.

4 "c" photometric confusion
Source photometry is biased by a nearby star that has contaminated the background estimation.

9 "s" electronic stripe
Source measurement may be contaminated by a stripe from a nearby bright star.

14 confusion in cross-band merge
This bit is set during the bandmerging process. The bandmerger reports, for each source and band, the number of merge candidates it considered in each of the other bands. If the number of candidates is greater than 2, then the bandmerger had to resolve the choice based on examination of the different band-pair combinations and position χ^2 differences between candidates. If the number of candidates is greater than 1, the confusion flag is set.

20 "d" diffraction spike confusion
Source may be contaminated by a diffraction spike from a nearby star.

22 post-lumping in cross-band merge
This bit is set for all bands (IRAC and 2MASS) if the source is a result of sources that were lumped in the cross-band merge step. Cross-band lumping is done with a 1.6″ radius.

23 Photometric quality flag
24 Photometric quality flag
25 Photometric quality flag

```
  2MASS            SQF bits
"ph" Flag  =>    23, 24, 25      value
-------------  --------------- ----------
   X              0   0   0           0
   U              1   0   0     4194304
   F              0   1   0     8388608
   E              1   1   0    12582912
   D              0   0   1    16777216
   C              1   0   1    20971520
   B              0   1   1    25165824
   A              1   1   1    29360128

 where
```

```
X - There is a detection at this location, but no valid brightness estimate can be
     extracted using any algorithm.

U - Upper limit on magnitude. Source is not detected in this band or it is detected,
     but not resolved in a consistent fashion with other bands.

F - This category includes sources where a reliable estimate of the photometric
     error could not be determined.

E - This category includes detections where the goodness-of-fit quality of the
     profile-fit photometry was very poor, or detections where psf fit photometry
     did not converge and an aperture magnitude is reported, or detections where
     the number of frames was too small in relation to the number of frames in
     which a detection was geometrically possible.

D - Detections in any brightness regime where valid measurements were made
     with no [jhk]_snr or [jhk]_cmsig requirement.

C - Detections in any brightness regime where valid measurements were made
     with [jhk]_snr>5 AND [jhk]_cmsig<0.21714.

B - Detections in any brightness regime where valid measurements were made
     with [jhk]_snr>7 AND [jhk]_cmsig<0.15510.

A - Detections in any brightness regime where valid measurements were made
     with [jhk]_snr>10 AND [jhk]_cmsig<0.10857.
```

B.3 Key to Bit Values

This section describes how to determine the bit values of a Source Quality Flag.

bt = bit in sqf
value = $2^{(bit-1)}$ i.e. bit 3 corresponds to 2^2=4

bit values: bt 1 => 1; 2 => 2; 3 => 4; 4 => 8; 5 => 16; 6 => 32; 7 => 64; 8 => 128 bt 9 => 256; 10 => 512; 11 => 1024; 12 => 2048; 13 => 4096; 14 => 8192; 15 => 16384; bt 16 => 32768; 17 => 65536; 18 => 131072; 19 => 262144; 20 => 524288; bt 21 => 1048576; 22 => 2097152; 23 => 4194304; 24 => 8388608; 25 => 16777216; 30 => 536870912

For example, the Source Quality Flags in the example in Table 9 are 29360128 for the 2MASS J band and 25165824 for the H and K_s bands. This translates to bits 23, 24 and 25 being set for J, which is the photometric quality A flag from the 2MASS PSC. For H and K_s, bits 24 and 25 are set meaning the photometric quality flag is B. IRAC [3.6] has a SQF of 1536. This means bits 10 and 11 have been set which means the tweaking has been done in the source extraction. IRAC [4.5] SQF is 17408. This means bits 11 and 15 were set which means tweaking was done in the source extraction and the source is within three pixels of a column pulldown corrected area.

9 APPENDIX C - Examples of Artifacts in the Images

Many Spitzer image artifacts are corrected for in our data pipeline. We correct for column pull-down[12] in the [3.6] and [4.5] bands using an algorithm written by Matt Ashby and Joe Hora of the IRAC instrument team [13] and modified by GLIMPSE to handle variable backgrounds. Hot, dead, and missing pixels are masked. Outlier masking (e.g. cosmic rays, stray light from bright sources outside the field of view) was done using IRACproc (Schuster et al 2006). Instrument artifacts (e.g. stray light) found by visual inspection of the higher resolution $0.6''$ mosaics were removed. Latent images from bright sources are removed when possible. If there are areas of overlapping image artifacts that cause a gap in coverage, we do not mask that area. Latent images can repeat (particularly along rows and columns) and remain in the images because masking them would cause gaps in coverage. Some instrument artifacts near the edge of coverage cannot be removed without causing gaps in the images, because of little or no redundancy of coverage. Background matching and gradient correction mostly remove image artifacts such as full array pull-up, frame pull-down and offsets between the AORs. The background matching and gradient correction may be removing real sky variations so we provide the corrected images in addition to the images that do not have the background matching. This Appendix gives examples of instrument artifacts that can still be found in the images after the outlier masking was done and after some stray light areas were removed as a result of the visual inspection (Figures 13 through 19). See SSC's IRAC image features web sites[14], [15] and the IRAC Data Handbook for more information about the detector artifacts. We also show an example (Figure 20) of some detector artifacts in the WISE [12] images since we are using the WISE images in our quick-look 3-color jpegs. For more information about the WISE image artifacts, see http://wise2.ipac.caltech.edu/docs/release/allsky/expsup/sec2_3c.html. If Figures 13 through 20 don't print well, they may be more clear when viewed on a computer screen.

[12] Column pulldown is a reduction in intensity of the columns in which bright sources are found in the [3.6] & [4.5] bands

[13] irsa.ipac.caltech.edu/data/SPITZER/docs/dataanalysistools/tools/contributed/irac/fixpulldown/

[14] irsa.ipac.caltech.edu/data/SPITZER/docs/irac/features/

[15] irsa.ipac.caltech.edu/data/SPITZER/docs/irac/warmfeatures/

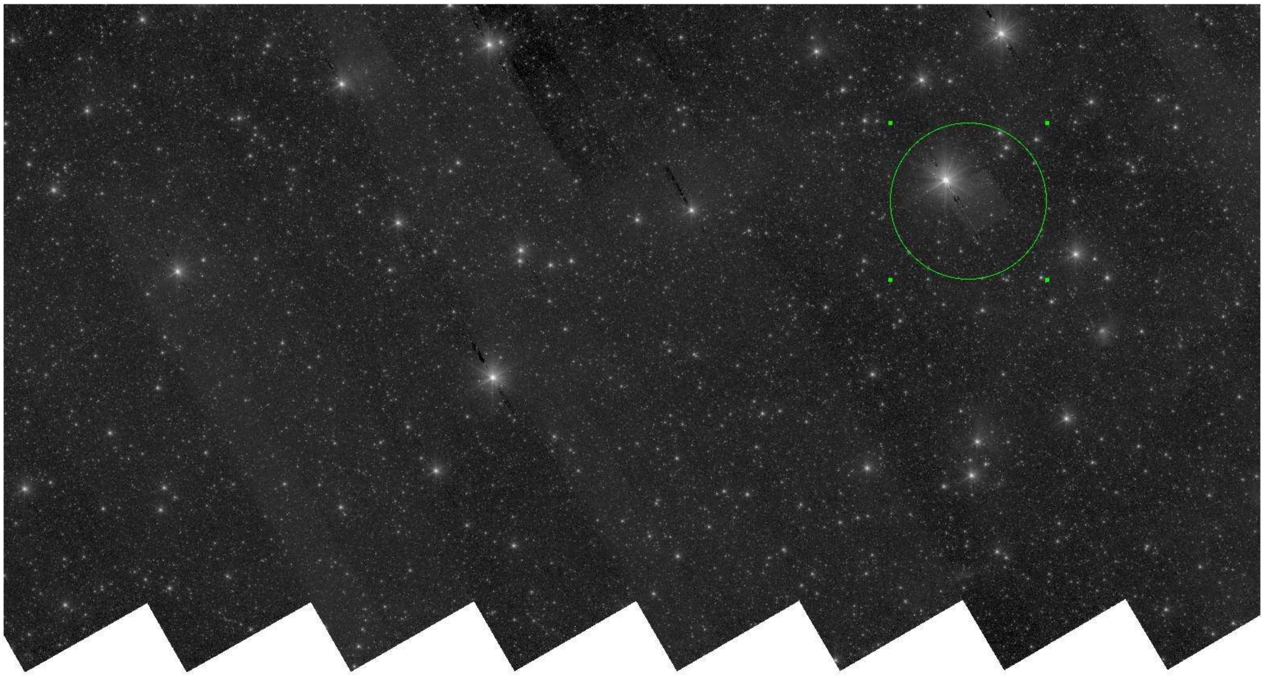

Figure 13: Example of offsets between AORs and full array pull-up near a bright source (circled) in an IRAC [3.6] image (centered at l=153.0°, b=-0.25°) which has not been background matched and gradient corrected.

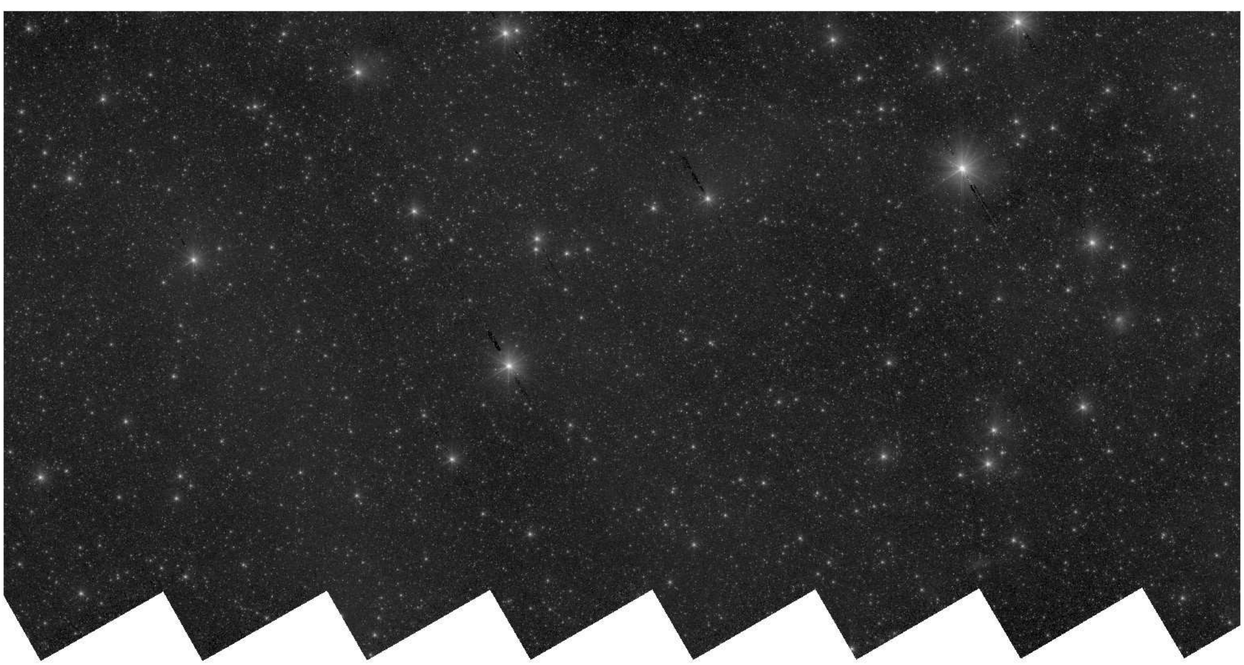

Figure 14: Example of the same area shown in Figure 13, with background matching and gradient correction applied. The offsets between the AORs have been improved and the full array pull-up near the bright source has been mitigated.

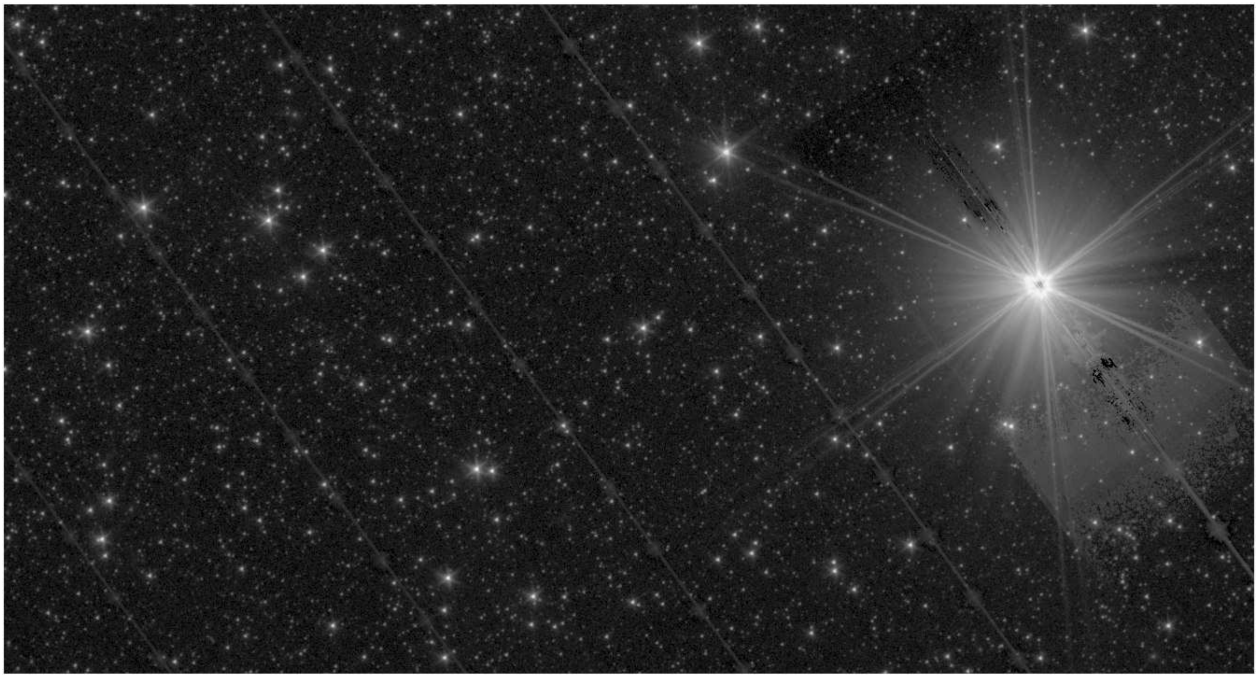

Figure 15: Example of latents (from the bright object on the right) in an IRAC [3.6] image (centered at l=165.2°, b=-0.45°). There are also full array pull-ups near the bright source.

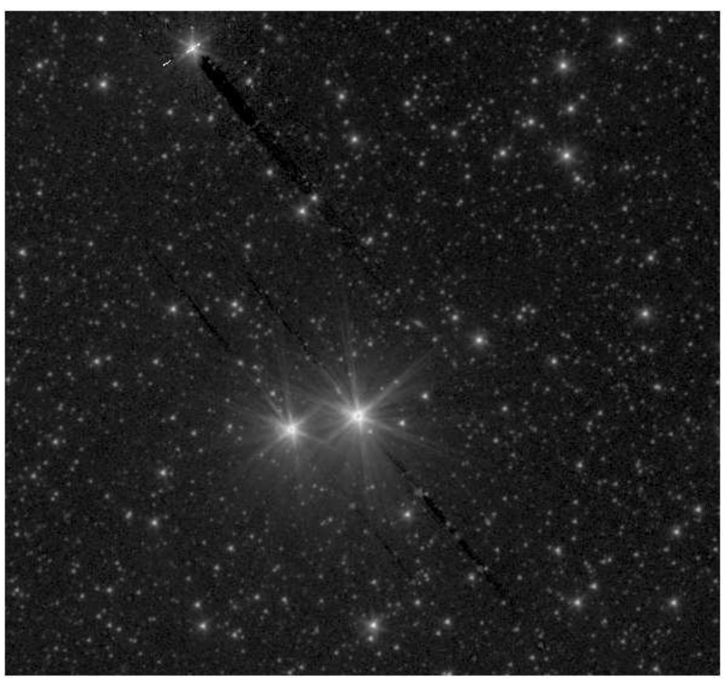

Figure 16: Example of column pull-down in an IRAC [3.6] image centered at l=164.35°, b=+0.76°.

Figure 17: Example of pull-down latents in an IRAC [4.5] image centered at l=165.2°, b=-0.45°. Also note the frame pull-up near the bright source on the right.

Figure 18: Example of column pull-ups in an IRAC [4.5] image centered at l=135.73°, b=+0.92°.

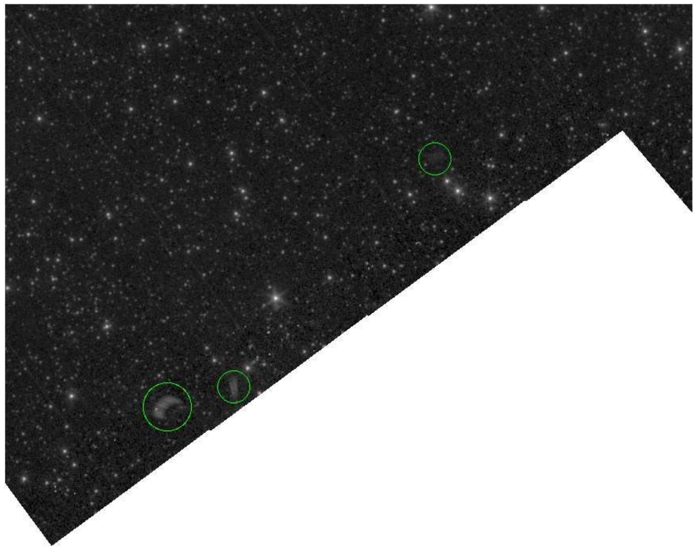

Figure 19: Example of stray light areas (circled) near the edge of coverage in an IRAC [4.5] image centered at l=144.5°, b=-0.85°. Since there are fewer visits at the edge the stray light areas cannot be masked without causing gaps in coverage. Note also a few column pull-up areas.

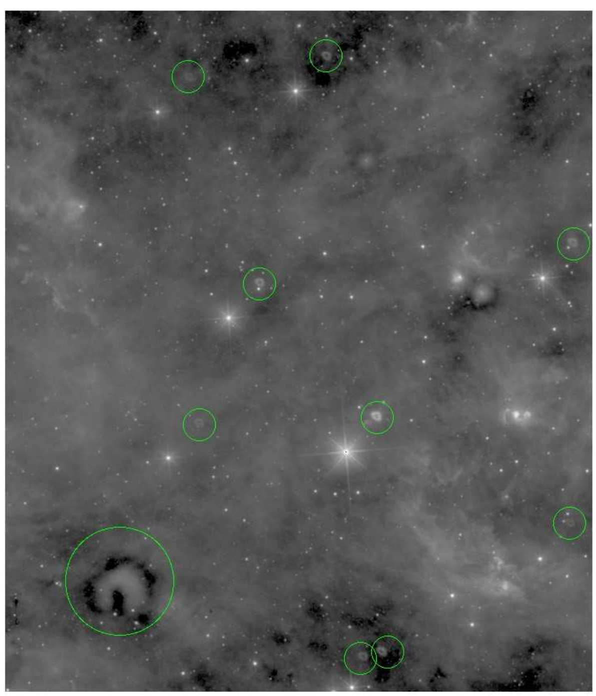

Figure 20: Example of latents (circled) in a WISE [12] image centered at l=125.6°, b=+0.44°.

10 REFERENCES

Aguirre, J., et al. 2011, ApJS, 192, 4.
Araya, E., Hofner, P., Churchwell, E.,and Kurtz, S. 2002, ApJS, 138, 63.
Benjamin, R.A. et al. 2003, PASP, 115, 953.
Benjamin, R.A. et al. 2005, ApJ, 630, L149.
Benjamin, R.A. et al. 2007, AIPC, 943, 101
Binney, J. & Merrifield, M. 1998, Galactic astronomy (Princeton) 635.
Calabretta, M.R. and Greisen, E.W. 2002, A & A, 395, 1077.
Churchwell, E. et al. 2009, PASP, 121, 213.
Cohen, M., Wheaton, W.A., and Megeath, S.T. 2003, AJ, 126, 1090.
Cole, A. & Weinberg, M. 2002, ApJ 574, L43.
Cutri, R. et al. 2005, www.ipac.caltech.edu/2mass/releases/allsky/doc/sec2_2.html#pscastrprop.
Dickey, J. et al. 2010, ASPC, 438, 428.
Fazio, G.G. et al. 2004, ApJS, 154, 10.
Froebrich, D. et al. 2010, MNRAS, 413, 480.
Gerhard, O. 2002, ASPC, 273, 73.
Hammersley, P., et al. 2001, ASPC, 231, 81.
Heyer, M. et al. 1998, ApJS, 115, 241.
Hoare, M.G. et al. 2012, PASP, 124, 939.
Holland, W. et al. 2006, SPIE, 6275, 45.
Hora, J. et al. 2004, Proc SPIE, 5487, 77.
Ishihara, D. et al. 2010, A&A, 514, 1.
Jackson, J.M. et al. 2006, ApJS,163, 145.
Kaufman, M.J., Wolfire, M.G., Hollenbach, D.J., and Luhman, M.L. 1999, ApJ, 527, 795.
Kaufman, M.J., Wolfire, M. G., & Hollenbach, D. J. 2006, ApJ, 644, 283.
Kobulnicky, H.A. et al. 2013, ApJS, 207, 9.
Lucas, P. et al. 2008, MNRAS, 391, 136.
MacKenzie, T. et al. 2011, MNRAS, 415, 1950.
Minniti, D. et al. 2010, New Astronomy, Vol. 15, Issue 5, p. 433.
Molinari, S. et al. PASP, 2010, 122, 314-325.
Mottram, J.C. & Brunt, C.M., 2010, ASP Conference Series, Vol. 438, 98.
Price, S.D., et al. 2001, AJ, 121, 2819.
Reach, W. et al. 2005, PASP, 117, 978.
Robitaille, T., Whitney, B., Indebetouw, R., Wood, K. & Denzmore, P. 2006, ApJS, 167, 256.
Robitaille, T., Whitney, B., Indebetouw, R., & Wood, K. 2007, ApJS, 169, 328
Schuster, M. T., Marengo, M., & Patten, B. M. 2006, Proc SPIE, 6270, 65.
Skrutskie, M.F. et al. 2006, AJ, 131, 1163.
Stanimirovic, S., et al. 2006, ApJ, 653, 1210.
Stetson, P. 1987, PASP, 99, 191.
Taylor, J. & Cordes, J. 1993, ApJ, 411, 674
Tielens, A.G.G.M. and Hollenbach, D.J. 1985, ApJ, 291, 722.
Watson, C., Araya, E., Sewilo, M., Churchwell, E., Hofner, P., and Kurtz, S. 2003, ApJ, 587, 714.
Werner, M.W. et al. 2004, ApJS, 154, 1.
Whitney, B.A. et al., 2003a, ApJ, 591, 1049.
Whitney, B.A. et al., 2003b, ApJ, 598, 1079.
Whitney, B.A. et al., 2004, ApJ, 617, 1177.

Wolfire, M.G. and Cassinelli, J.P. 1986, ApJ, 310, 207.
Wolfire, M.G., Tielens, A.G.G.M., and Hollenbach, D.J. 1990, ApJ, 358, 116.
Wright, E.L. et al. 2010, AJ, 140, 1868.

GLOSSARY

2MASS	Two Micron All Sky Survey
ATLASGAL	The APEX Telescope Large Array Survey of the Galaxy
BGPS	Bolocam Galactic Plane Survey
BCD	Basic Calibrated Data, released by the SSC
CORNISH	Coordinated Radio and Infrared Survey for High-Mass Star Formation
DIRT	Dust Infrared Toolbox, for data analysis
dmask	A data quality mask supplied by the SSC for the BCD
FCRAO	Five-College Radio Astronomy Observatory
GALFA	Galaxy ALFA Low Latitude HI Survey
GASKAP	Galactic Australian SKA Pathfinder Survey
GBT	Green Bank Telescope (100 m)
GLIMPSE	Galactic Legacy Infrared Midplane Survey Extraordinaire
GLM360C	GLIMPSE360 Point Source Catalog
GLM360A	GLIMPSE360 Point Source Archive
GRS	Galactic Ring Survey (^{13}CO)
HI-GAL	Herschel Infrared Galactic Plane Survey
IGPS	International Galactic Plane Survey
IPAC	Infrared Processing and Analysis Center
IRAC	*Spitzer* Infrared Array Camera
IRS	*Spitzer* Infrared Spectrometer
IRSA	InfraRed Science Archive
MF	Method Flag used to indicate exposure times included in the flux
MIPS	*Spitzer* Multiband Imaging Photometer
MSX	Midcourse Space Experiment
NRAO	National Radio Astronomy Observatory
PDR	Photodissociation Region
PDRT	PhotoDissociation Region Toolbox, for data analysis
pmask	A bad pixel mask supplied by the SSC for the BCD
PSF	Point Spread Function
rmask	Outlier (radiation hit) mask
SCUBA-2	Submillimetre Common-User Bolometer Array 2
SOM	*Spitzer* Observer's Manual
SSC	*Spitzer* Science Center
SED	Spectral energy distribution
SQF	Source Quality Flag
SST	*Spitzer* Space Telescope
UKIDSS	UKIRT Infrared Deep Sky Survey
UWISH2	UKIRT Widefield Infrared Survey for H2
VLA	Very Large Array
VVV	Vista Variables in the Via Lactea
YSO	Young Stellar Object
WISE	Wide-field Infrared Survey Explorer
WITS	Web Infrared Tool Shed, for data analysis